

**IDENTIFICATION OF BLUE STRAGGLERS
IN THE GLOBULAR CLUSTER M53 USING
CCD PHOTOMETRY**

H.M.U. KAUSHAL

S/09/660

Department of Physics, Faculty of Science, University of Peradeniya- 2014

IDENTIFICATION OF BLUE STRAGGLERS IN THE GLOBULAR
CLUSTER M53 USING CCD PHOTOMETRY

A PROJECT REPORT PRESENTED BY
H.M.U. KAUSHAL

*In partial fulfillment of the requirement
for the award of the degree of*

B.Sc. (Physics Special)
of the

Faculty of Science,
University of Peradeniya,

Sri Lanka

2013/2014

ACKNOWLEDGEMENT

First and foremost, I would like to convey my heartfelt gratitude to my supervisors Dr. T. Ranawaka, Senior Lecturer, University of Peradeniya and Mr. S. Gunasekara, Senior Research Scientist, Arthur C. Clarke Institute for Modern Technologies, for their invaluable guidance given to me throughout my research.

My profound thanks also goes to Mr. J. Adassuriya, Research Scientist, Arthur C. Clarke Institute for Modern Technologies, for providing me with the observational data used in this research and also for his immense support.

I am grateful to the staff at Mount Abu Observatory, Girishikar, India for letting me use data obtained through their telescope.

Finally, to my family and all my colleagues who were always willing to help, I extend you my sincere appreciation.

ABSTRACT

THE IDENTIFICATION OF BLUE STRAGGLERS IN THE GLOBULAR CLUSTER M53 USING CCD PHOTOMETRY

CCD observational data of the globular cluster M53 (NGC5024), obtained with the 1.2 m telescope at Mount Abu Observatory, Girishikar, India have been reduced and analyzed. The software package IRAF was utilized for that purpose. Both aperture photometry and psf-fitting photometry methods were experimented. A B-V passband color-magnitude diagram for the cluster which extends below $V=21$ is presented using more than 2000 stars. The main sequence turn off point of the cluster was found to be $V_{TO}=18.43 \pm 0.06$ and $(B - V)_{TO} = 0.449 \pm 0.064$ which is in agreement with previous research literature. The distance modulus of the cluster was found to be 14.53 ± 0.23 which is also quite consistent with previous results. The distance to the cluster was calculated to be 8.05 kpc. An approximate value was estimated for the age of the galaxy which turned out to be at least 3.2Gyr. 19 Blue Straggler Stars have been identified in the cluster.

TABLE OF CONTENTS

	Page
Title	i
Acknowledgement	ii
Abstract	iii
Table of Contents	iv
List of Figures	vi
List of Tables	ix
CHAPTER 01: INTRODUCTION	1
CHAPTER 02: STELLAR CLASSIFICATION	3
2.1 Black Body Spectrum of stars	6
2.2 Hertzsprung-Russel Diagrams (HR Diagrams)	7
2.3 Color-Magnitude Diagram (CMD)	8
2.4 Blue Straggler Stars (BSS)	9
CHAPTER 03: GLOBULAR CLUSTERS	12
3.1 M53	13
CHAPTER 04: PHOTOMETRY	15
4.1 The magnitude scale	15
4.2 Photometry	16
4.2.1 Measuring Photometry from Images	16
4.3 Filters	18
4.4 IRAF	19
CHAPTER 05: OBSERVATIONAL DATA	20
CHAPTER 06: CCD IMAGE PROCESSING	22
6.1 Charged Coupled Devices	22
6.1.1 Working Principle	22

6.2 Image Format	24
6.3 Data Reduction	26
6.3.1 Data Reduction Procedure	27
6.4 Data Analysis	27
CHAPTER 07: APERTURE PHOTOMETRY	30
7.1 Data Analysis	31
CHAPTER 08: PSF FITTING PHOTOMETRY	33
8.1 Aperture corrections	34
8.2 Data Analysis	34
CHAPTER 09: STANDARD MAGNITUDE CALIBRATION	37
9.1 Extinction and Airmass	37
9.1.1 Data Analysis	38
9.2 Transformation Equations	38
9.2.1 Data Analysis	39
CHAPTER 10: UNCERTAINTIES	41
CHAPTER 11: RESULTS AND ANALYSIS	42
11.1 Aperture Photometry Results	42
11.1.1 Aperture Radius= 10 px	42
11.1.2 Aperture Radius= 7 px	43
11.1.3 Aperture Radius= 3 px	43
11.2 PSF- Fitting Photometry Results	44
11.3 Analysis	44
11.4 Conclusion	45
REFERENCES	46
APPENDIXES	47

LIST OF FIGURES

	Title	Page
Figure 2.1	The absorption lines corresponding to each stellar class	4
Figure 2.2	The black body radiation curve	6
Figure 2.3	The typical HR diagram	7
Figure 2.4	The typical color magnitude diagram for a globular cluster	8
Figure 2.5	The CMD of M3	10
Figure 2.6	A CMD of M30 displaying two sequences of BSS	10
Figure 2.7	Formation of Blue Stragglers	11
Figure 3.1	The globular cluster M53	13
Figure 3.2	The finder chart for M53	14
Figure 4.1	Airy's disk pattern	17
Figure 4.2	Observed image of a point star	17
Figure 4.3	Image formation of a point star	17
Figure 4.4	Resultant Gaussian Function	17
Figure 4.5	The Johnson-Cousin filter system wavelength response	18
Figure 4.6	The IRAF system	19
Figure 5.1	The HAWAII-1 1kx1k CCD detector	20
Figure 5.2	The Mount Abu Observatory and its telescope	21

Figure 6.2	A schematic diagram of a CCD pixel	22
Figure 6.3	The action of a CCD	23
Figure 6.4	The response curve for the KAF-4200 CCD	24
Figure 6.5	The pixel matrix of an image	25
Figure 6.6	The header of a FITS file	25
Figure 6.7	The bias frame	27
Figure 6.8	The flat frame	27
Figure 6.9	The M53 object frame in V filter before reduction	28
Figure 6.10	The pixel value vs. column plot for M53 in V before reduction	28
Figure 6.11	The M53 object frame in V filter after reduction	29
Figure 6.12	The pixel value vs. column plot for M53 in V after reduction	29
Figure 7.1	Using an aperture and annulus for aperture photometry	30
Figure 7.2	The radial plot of a V band star	31
Figure 7.3	The radial plot of a B band star	31
Figure 7.4	Detected stars in the V band	32
Figure 7.5	Detected stars in the B band	32
Figure 8.1	A modeled psf	33
Figure 8.2	A “good” psf model	34
Figure 8.3	A defective psf model	34
Figure 8.4	The psf subtracted V field	34
Figure 8.5	The psf subtracted B field	34
Figure 8.6	The Curve of Growth for the V band	35
Figure 8.7	The Curve of Growth for the B band	35

Figure 9.1	The airmass of the atmosphere	37
Figure 9.2	Aladin standard star locator	39
Figure 9.3	The graph of V (catalog) vs v (instrumental)	40
Figure 9.4	The graph of B (catalog) vs b (instrumental)	40
Figure 10.1	Aperture photometry mag error	41
Figure 10.2	PSF photometry mag error	41
Figure 11.1	The CMD of M53 for 10px aperture	42
Figure 11.2	The CMD of M53 for 7px aperture	43
Figure 11.3	The CMD of M53 for 3px aperture	43
Figure 11.4	The CMD of M53 using PSF-Fitting photometry	44

LIST OF TABLES

	Title	Page
Table 3.1	Properties of the globular cluster M53	14
Table 5.1	The table containing observational data	21
Table 7.1	The average FWHM and sky values	32
Table 8.1	The aperture correction values	36
Table 9.1	Airmasses calculated for the B and V filters	38
Table 11.1	Summary of obtained values	45

CHAPTER 01

INTRODUCTION

Galaxies in the universe, including the Milky Way, consist of a vast collection of star clusters. As the name suggests, a star cluster is a group of stars clumped closely together. There are two types of star clusters, namely open clusters and globular clusters. Open clusters like the Pleiades are relatively younger and are loosely bound by gravity. They reside in the spiral arms of the galaxy and contain a few hundred stars. Globular clusters on the other hand, are as old as the universe itself and are tightly bound by gravity. This type of cluster has a monolithic stellar density of about ten thousand to a million stars and resides in the bulge or the halo of a galaxy. M53 or Messier 53 is one such globular cluster ^[1].

Globular clusters possess a unique set of characteristics which make them worthy of studying. Their antiquity turns them into stellar clocks that establish a lower limit to the age of the universe ^[2]. All the stars in the cluster are of the same age and roughly the same distance away from us. The latter brings out the fact that the apparent magnitudes of the stars are nearly as viable measurements as their absolute magnitudes are. i.e. the stars that appear brighter are truly brighter in reality and vice versa. The result is a constant distance-modulus (the difference between absolute magnitude and apparent magnitude) for all the stars in the cluster. This gives a direct correlation between a star's Luminosity and its apparent magnitude, thus making it possible to construct meaningful HR (Hertzsprung-Russel) diagrams or CMDs (Color-Magnitude Diagrams) which are essentials in studying their nature ^[3].

Early studies of these diagrams obtained from clusters showed a handful of massive blue stars lying beyond the Main Sequence Turn-Off (MSTO) point; the point where the oldest stable star (a star fusing H into He) occupy the diagrams. Massive blue stars which have higher luminosities evolve off the main sequence sooner than their less-luminous members. The discovery of such stars were highly paradoxical since all the stars were of the same age, meaning these massive blue stars should already be dead. These peculiar stars were coined "Blue Straggler Stars" or BSS because they were left behind by other blue stars that evolved into Red Giants long ago. The formation of BSSs is a matter that is still widely debated ^{[4][5]}.

This research focuses on the globular cluster M53 also known as NGC 5024, a class V globular cluster situated in the constellation of Coma Berenices. It was discovered by Johann Elert Bode in 1775. Two years later, Charles Messier catalogued it. Sir William Herschel was the first person to resolve it into stars. The first photometric study of the cluster was carried out by Cuffey in 1965 where he obtained a B-V band photographic CMD for 569 stars which reached only 1.5 mag below the Horizontal Branch. In more recent studies, Soo-Chang Rey Young-Wook Lee, and Yong-Ik Byun & Mun-SukChun (1998) conducted a B-V band photometry of 20,000 stars covering a 12' x 13' region of the cluster using a large-format CCD in which they identified 114 BSSs ^[14].

Throughout the decades new technologies have emerged in astronomical photometry; the science of measuring the flux of photons. CCDs or charged coupled devices have replaced the outdated photo electric photometers. Unlike photometers, CCDs can deal with a multitude of objects at once. These CCDs, combined with state-of-the-art telescopes and modern computers have opened up new windows into the universe ^[7].

In this report, we present a multiband photometric study (aperture photometry and psf fitting photometry) of the globular cluster M53, performed with data obtained through the 1.2 meter telescope at Mount Abu Observatory, Girishikar, India. IRAF (Image Reduction and Analysis Facility) and Matlab running on a Linux Mint 17 system were utilized to analyze the data which ultimately led to the construction of the cluster's Color-Magnitude Diagram which was employed to study its stellar population.

CHAPTER 02

STELLAR CLASSIFICATION

In astrophysics, stars are classified by their surface temperature which is associated with their spectral characteristics. The spectral class of a star describes the ionization of its chromosphere, what atomic excitations are most prominent in the light, which is a measure of the temperature in the chromosphere. Light from the star is analyzed by splitting it with a diffraction grating into a spectrum consisting absorption lines. Each line indicates an ion of a chemical element, with the line strength indicating the abundance of that ion. The relative abundance of the different ions varies with the temperature of the photosphere.

The first classification scheme was compiled in the 1920's by the director of the Harvard College Observatory, E. C. Pickering, and his assistants, most notably Annie Jump Canon who cataloged nearly 200,000 stellar spectra. This was introduced as the Henry Draper Catalog which was based on the strengths of the Balmer absorption lines for Hydrogen and letters from A-P were assigned accordingly. Modern astrophysicists use the Morgan–Keenan (MKK) system, an extension of the previous, using the letters *O*, *B*, *A*, *F*, *G*, *K*, and *M*, a sequence from the hottest (*O* type) to the coolest (*M* type). Each letter class is then subdivided using a numeric digit with *0* being hottest and *9* being coolest (e.g. A7, A8, F0, F2 form a sequence from hotter to cooler).

The following is a description of each of the above discussed star classes.

- **Class O** stars are very hot and luminous, being blue in color. These stars have prominent ionized and neutral helium lines and only weak hydrogen lines. Class O stars emit most of their radiation in the ultra-violet region.
- **Class B** stars are also very luminous, Rigel is a B class blue supergiant. Their spectra have neutral helium and moderate hydrogen lines. As O and B stars are highly luminous, they live for a very short time.

In the MKK system a Luminosity class based on the width of the absorption lines in the star's spectrum is expressed using Roman numerals.

class *0* (Hypergiants)- The most massive stars that have been discovered so far. Extremely rare.

class *I* (Supergiants)- Very massive and luminous stars near the end of their lives. They are subclassified as Ia or Ib, with Ia being the brightest, according to their brightness. These stars are very rare; one in a million stars is a supergiant. The nearest supergiant star is Canopus (F0Ib) 310 light years away.

class *II* (Bright giants)- Stars which have a luminosity between the giant and supergiant stars. Examples are Sargas (F1II) and Alphard (K3II).

class *III* (Regular giants)- These are mainly low-mass stars at the end of their lives that have swelled to become a giant star. This category also includes high mass stars evolving to become supergiants. Examples are Arcturus (K2III), Hadar (B1III) and Aldebaran (K5III).

class *IV* (Sub-giants)- Stars which have begun evolving to giant or supergiant status. Examples are Alnair (B7IV) and Muphrid (G0IV).

class *V* (Main Sequence stars)- All hydrogen-burning stars. Stars spend most of their lives in this category before evolving up the scale. Class O and B stars in this category are very bright and luminous and are generally brighter than most Giant stars. Examples are the Sun (G2V), Sirius (A1V), and Vega (A0V).

class *VI* (Sub-dwarfs)- Stars that have properties between main-sequence stars and white dwarfs.

class *VII* (White dwarfs)- A small, very dense, hot star that is made mostly of Carbon. These faint stars are what remains after a red giant star loses its outer layers. Their nuclear cores are depleted. They are about the size of the Earth. They will eventually lose their heat and become a cold, dark black dwarf. Our sun will someday turn into a white dwarf and then into a black dwarf. The companion of Sirius is a white dwarf.

class *VIII* (Brown dwarfs)- A star whose mass is too small to have nuclear fusion occur at its core. A brown dwarf is not very luminous.

2.1 Black Body Spectrum of stars

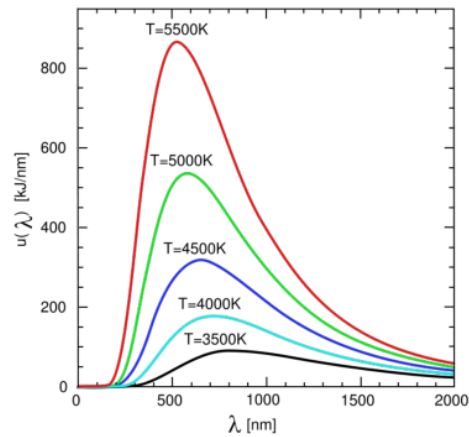


Figure 2.2 The black body radiation curve

In photometry, a useful relationship between the color of a star and its temperature is given by Wien's Law. Here, it is assumed that the star behaves as a black body.

$$\lambda_{max} \times T = 0.002897755 \text{ mK}$$

where,

λ_{max} -Wavelength of peak emission

T- Temperature

Furthermore, to determine a star's Luminosity, which is the energy radiated per unit time from the star, Stephan's Law can be employed.

$$L = 4\pi R^2 \sigma T^4$$

Where,

R- Radius of the star

T- Surface Temperature of the star

σ - Stephan's Constant

2.2 Hertzsprung-Russel Diagrams (HR Diagrams)

The Hertzsprung -Russell Diagram or HR diagram (Figure 2.3) is a scatter graph that plots a star's Luminosity or absolute magnitude vs. spectral type or surface temperature. This diagram features three main regions.

- (1) Most stars, including the Sun, are Main Sequence Stars, fueled by nuclear fusion converting Hydrogen into Helium. They are stable. This stage generally lasts for about 5 billion years.
- (2) As stars begin to die, they become giants and supergiants and move to a region above the Main Sequence. These stars have depleted their hydrogen supply and are very old. The core contracts as the outer layers expand. These stars will eventually explode and then become white dwarfs, neutron stars, or black holes depending on their mass.
- (3) Smaller stars eventually become faint white dwarfs and move to a region beneath the Main Sequence. These stars have depleted their nuclear fuel and will eventually become cold, dark black dwarfs.

The HR diagram contains information about the mass, radius, lifetime, distance, temperature, spectral type, luminosity of stars.

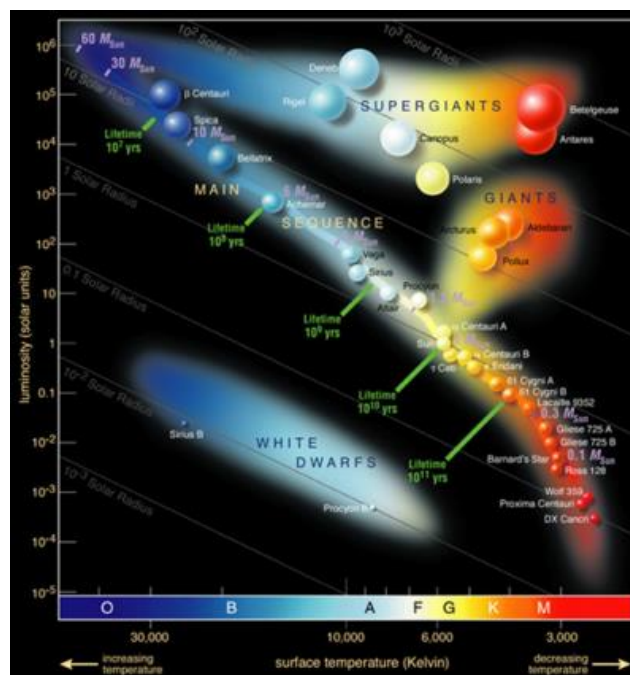


Figure 2.3 The typical HR Diagram

2.3 Color-Magnitude Diagram (CMD)

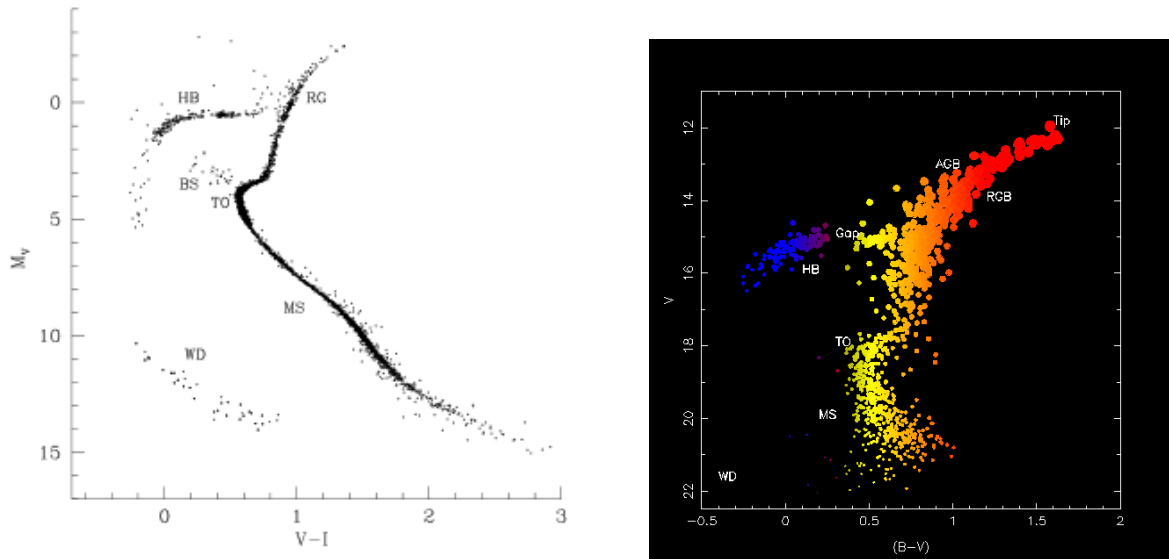


Figure 2.4 The typical color magnitude diagram for a globular cluster

The color-magnitude diagram is a variant of the HR diagram which is plot for star clusters. The plot is between absolute of apparent magnitude with the color index, which is the difference of magnitudes through two different filters. This is valid as all the stars in the cluster are effectively at the same distance away from us hence any differences in apparent magnitude are due to actual difference in luminosity. These are equivalent to plots of luminosity vs. temperature.

The regions of main phases of stellar evolution in a globular cluster is shown in Figure 2.4 and are explained below.

- **The Main Sequence (MS)** - this is where stars spend most of their lifetime consuming hydrogen in their cores via nuclear fusion. Our Sun currently resides on the main sequence.
- **Turn Off (TO)** - As the hydrogen fuel in a star's core runs out, the core begins to collapse due to gravity and the star moves away from the main sequence. At this point nearly all the central fuel is gone.

- **Red Giant Branch (RGB)** - When the central fuel is gone, hydrogen starts to burn in an envelope around a dense helium core. The star's outer regions expand due to this new energy supply. As the emitting surface area of the star's photosphere increases so does its apparent brightness. As it expands, the photosphere cools (as it becomes cooler, the star becomes redder). The star thus moves up and to the right on the H-R diagram, climbing up the Red Giant Branch (RGB).
- **Helium Flash** - At the tip of the RGB the helium rich core ignites and helium fusion begins. This ignition of the core causes the star to move down the H-R diagram towards the Horizontal Branch region rapidly.
- **Horizontal Branch (HB)** - the HB is the region occupied by stars which burn helium in their cores, converting it into carbon. A feature of the HB in this particular globular cluster, M53, is a Gap in the HB.
- **Gap in HB** -The HB is separated into two sections - a blue HB and a red HB - separated by a gap. The gap indicates a region of instability in the physics of the stellar envelope which results in stars in this region quickly evolving either onto the red or blue parts of the HB. HB morphology differs between globular clusters, some globular clusters show both Blue and Red HB while some show just one type.
- **Asymptotic Giant Branch (AGB)** - As the central helium fuel runs out, shell burning starts again around the core. But, this time two shells are formed, the inner one burning helium and the outer burning hydrogen. The star now moves off the HB and up the Asymptotic Giant Branch (AGB) blowing off its outer layers.
- **White Dwarf (WD)** - Loss of the complete envelope of the star on the AGB leaves the central hot white dwarf in the middle of a planetary nebula.

2.4 Blue Straggler Stars (BSS)

Blue stragglers (BSS) are main sequence stars in open or globular clusters that are more luminous and bluer than stars at the main-sequence turn-off point for the cluster. Blue stragglers were first discovered by Allan Sandage in 1953 while performing photometry of the stars in the globular cluster M3 ^[8].

Stars spend most of their lives burning hydrogen in their cores and hence belong to the Mains Sequence. More massive stars lie at higher luminosities and they also use up their

hydrogen fuel and evolve off the main sequence faster than less luminous ones. In clusters, all the stars form at roughly the same time. As the cluster ages, fewer and fewer of its stars will be found on the main sequence. The point where the oldest stable star on the main sequence, the main-sequence turn-off can reveal the age of the cluster. If all stars in a cluster were to proceed through their lives the way models of single star evolution tell us they should, there should be no stars above the main sequence turn off. That portion of the HR diagram should be empty. However observations say otherwise. Handfuls of blue stars which lie above the turn-off have been discovered. These stars were named Blue Stragglers.

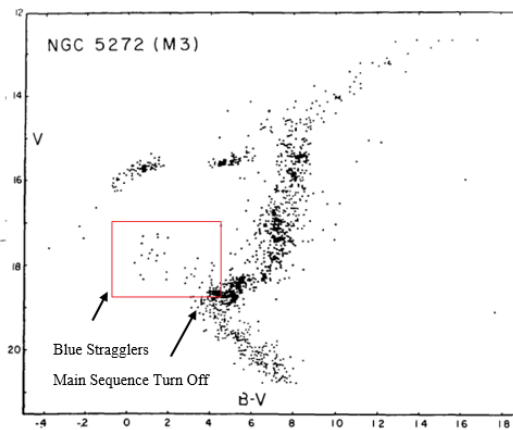


Figure 2.5 The CMD of M3^[11]

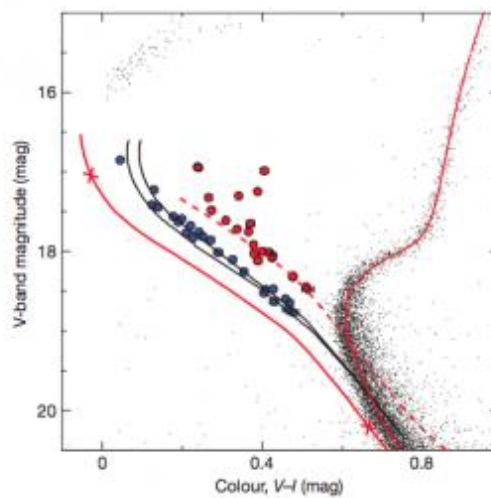


Figure 2.6: A CMD of M30 displaying two sequences of BSS

The location on the HR diagram implies that they have a particular mass. But, if they had been born with that mass then they should have already evolved off the main sequence. Therefore, they must have gained additional mass recently. Two main mechanisms for this have been proposed: (i) mass transfer within a binary system and (ii) the merger of two (or more) stars. (Figure 2.7) In a study conducted by E. Dalessandro, F. R. Ferraro, D. Massari et al. on the globular clusters M30 (2009) and NGC362 (2013), they identified two distinct parallel bands of BSSs beyond the MS, supposedly due to these two mechanisms. (Figure 2.6) This solidified the evidence behind the hypothesis ^[9].

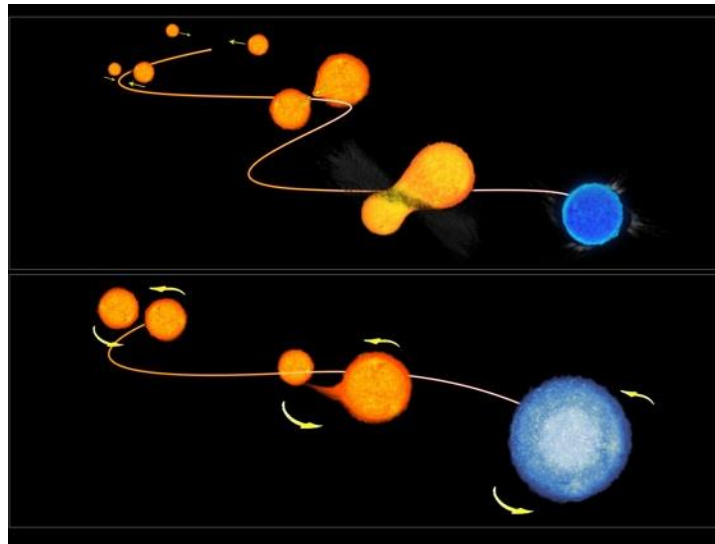


Figure 2.7: Formation of Blue Stragglers

Figure 2.7 demonstrates the two ways that blue stragglers in globular clusters form. The upper illustration shows the merger model where two low-mass stars in an overcrowded environment experience a head-on collision, combining their fuel and mass and to form a single young, hot star. The lower illustration depicts the mass-transfer model consisting of a pair of stars that undergo a transformation, with the lower mass star draining its larger mass companion of hydrogen that fuels its rebirth.

CHAPTER 03

Globular Clusters

Globular clusters are coalesced systems of about a million stars, gravitationally bound to each other. They take a symmetric spherical shape. So far about 160 globular clusters have been discovered in the Milky-way Galaxy. They are mainly found in the Halo of a galaxy. The stars of any one globular cluster share a common history (age, chemical abundance, etc) and differ one from the other only in their original mass. They thus form ideal candidates for the study of stellar evolution. In the following sections we will investigate how the observed colors and magnitudes of stars in the globular cluster M53 can be used to identify different stages in stellar evolution.

It is vital to study globular clusters for a number of reasons:

- The homogeneity of the stars in these clusters indicates that they have similar chemical compositions and similar ages. This makes them the simplest systems to use to test theoretical models of star formation and evolution.
- Globular clusters are some of the oldest stellar systems known and thus estimates of their ages can be used to estimate the lower age limit of the universe.
- The distribution of their ages, and correlations between cluster ages and metal abundances makes these systems an invaluable probe into the processes of galaxy formation.
- All stars are at the same distance from earth which give the direct measurability of absolute magnitude or apparent magnitude.

3.1 M53

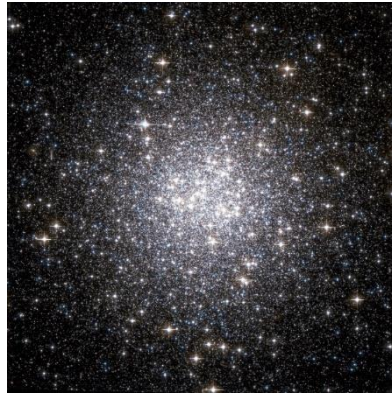


Figure 3.1 The globular cluster M53

Globular star cluster Messier 53 (M53, NGC 5024) is one of the more outlying GC's, being about 60,000 light years away from the Galactic center. Its stars are not very concentrated toward the center when compared to other GC's, and a gradually decreasing density profile to the outer edges. M53 is positioned in the eastern part of the constellation of Coma Berenices.

Its discoverer Johann Elert Bode, who found in 1775, described it as a "rather vivid and round" nebula. Charles Messier, who independently rediscovered and cataloged it two years later. William Herschel was the first to resolve it into stars.

As in all globular clusters, the stars of M53 are apparently "metal-poor", which means that they contain only little quantities of elements heavier than helium.

In small amateur telescopes, M53 appears as a slightly oval nebulous object with a large, bright center of rather even surface brightness and evenly fading out to the edges. In larger telescopes, its outer fringes appear resolved into stars, while the central part is still unresolved and grainy, with one star standing out, in telescopes of about 8-inch aperture. Large telescopes of about 12-inch and up show it well resolved, with a moderately concentrated nucleus and stars spread out to about 13 arc minutes diameter.

The cluster is quite easy to find (Figure 3.2), lying just 1 degree northeast of mag. +4.3 star Diadem. Located 15 degrees directly east of M53 is orange giant star Arcturus (mag -0.05), the fourth brightest star in the night sky. M53 is best seen from northern latitudes during the months of March, April and May.

Messier Finder Chart for M3, M53 and M64 Black Eye Galaxy

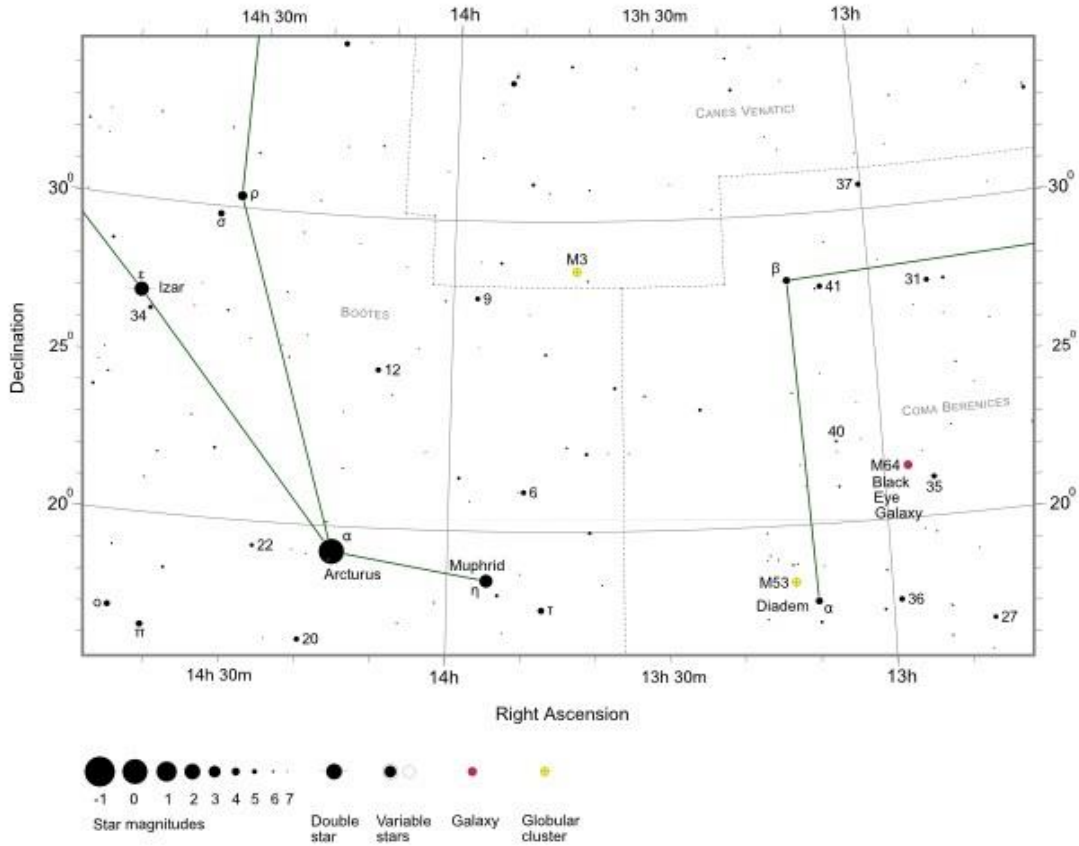


Figure 3.2 The finder chart for M53

Table 3.1

Properties of the globular cluster M53 ^[6]

Parameter	Value
Right Ascension	13h 12m 55.25s
Declination	+18° 10' 05.4"
Apparent Magnitude	+8.33
Diameter	220 LY
Mass	$8.26 \times 10^5 M_{\odot}$
Apparent Dimension	13 arcmin
Class	V

CHAPTER 04

PHOTOMETRY

4.1 The magnitude scale

In astronomy, fluxes are measured in magnitudes. The early stellar magnitude system was established by a Greek named Hipparchus 2200 years ago, who classified stars into magnitudes numbered 1 through 6 based on only the stars the human eye can see. Later it was discovered that they resembled a logarithmic scale. Two objects that differ in measured flux by a factor of 100 are defined as having 5 magnitudes difference. Thus, each magnitude is $100^{1/5}$ times as bright as the next.

The magnitude measured by an observer on earth is known as the apparent magnitude and is given by;

$$\text{Apparent Magnitude (m)} = -2.5\log(\text{flux}) + z_0$$

where;

$$\text{flux} = \frac{\text{counts (in ADU's)}}{\text{Exposure time}}$$

z_0 = zero point constant

d = distance between object & earth

The Absolute Magnitude (M) is defined as the magnitude of a star when it is at a distance 10pc from the observer and is given by;

$$m - M = 5\log d - 5$$

where, d is the distance to the star in parsecs.

Astronomers often refer to instrumental magnitudes, where the value of z_0 is not tied to a well-defined set of standards. Standard star calibration is required to convert the instrumental magnitude into standard magnitude. (discussed in a later chapter)

4.2 Photometry

Photometry is the science of measuring the flux from a celestial object. Usually, photometry refers to measurement over large wavelength bands of radiation. Basically, photometry is conducted by gathering radiation in a telescope, passing it through specialized optical filters and then measuring the light energy with a photosensitive instrument. The set of passbands (filters) is called a photometric system. For an example, only the red color (red wavelength) passes through a red filter.

Historically, photometry was done with a photoelectric photometer, an instrument that measured the light intensity of a single object by directing its light on to a photosensitive cell. They have now been replaced with charged couple devices (CCD), cameras which can simultaneously image multiple objects. In CCD, the intensity of wave converts to voltages in a capacitor array, and this voltage again converts to charge packets in a photoactive material (epitaxial layer of silicon). Finally this charge in photoactive material is dumped into a charge amplifier, which converts the charge into a voltage. This is then converted to digital units.

After determining the flux of an object in counts in different filters, one must calibrate the measurement in some way. To do this, one must correct measurements for changes in the sensitivity of the instrument as well as changes in the atmospheric extinction through which the object is observed. This is typically done by simultaneously observing a number of standard stars which have known magnitudes.

4.2.1 Measuring Photometry from Images

When the light from an astronomical point source is brought to a focus at the focal plane of a telescope, ideally we would see a diffraction-limited image, with Airy's rings (Figure 4.1) characterized by the Rayleigh Criterion;

$$\theta = \frac{1.22\lambda}{D}$$

where, θ - angular radius of the first dark ring

λ - wavelength of incident light

D- aperture diameter

In reality both the atmosphere and the telescope optics degrade the image to something that is more like a 2-dimensional Gaussian profile (Figure 4.2,4.4). The 2-d function that describes the light distribution in the focal plane that comes from a point source is called the Point Spread Function, or PSF. Clearly, the integral of the flux under the PSF is proportional to the flux received from the source.

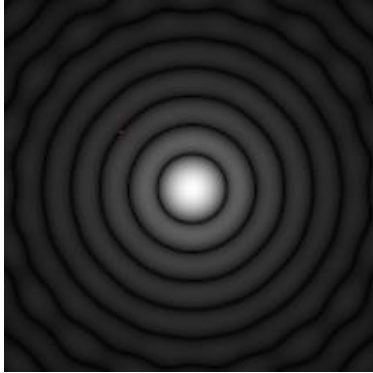


Figure 4.1 Airy's disk pattern

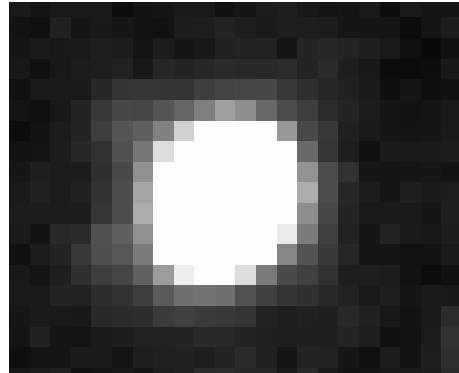


Figure 4.2 Observed image of a point star

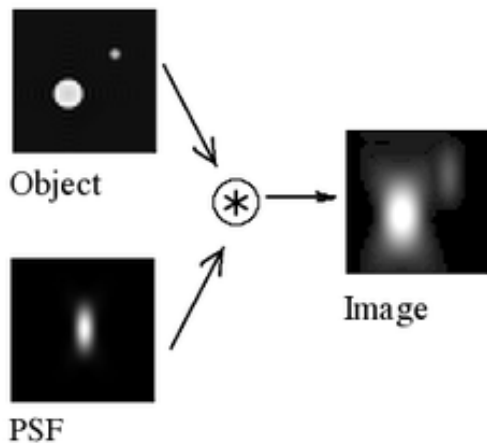


Figure 4.3 Image formation of a point star

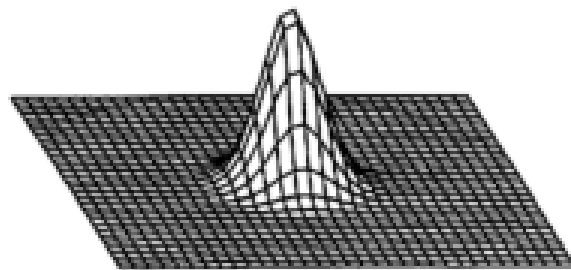


Figure 4.4 Resultant Gaussian Function

Mathematically, the image is the convolution of the object (f) with the PSF (h) which can be written as,

$$g(x,y) = \iint_{-\infty}^{\infty} h(x,y; \alpha, \beta) f(\alpha, \beta) d\alpha d\beta + \eta(x,y)$$

where,

$\eta(x,y)$ - the additive noise function

$f(\alpha, \beta)$ -the object

$g(x,y)$ -the image

$h(x,y; \alpha, \beta)$ - the Point Spread Function (PSF)

There are two common techniques to measure the flux of an object:

- (1) Aperture Photometry
- (2) PSF-fitting photometry

In Aperture Photometry a circular aperture is placed around the star of interest and the flux from the object that is within the aperture is integrated. This works well if the stars are well separated so that only the flux from a single object appears in the aperture. (discussed later)

For crowded fields aperture photometry does not work very well. The stellar images blend together, and any given pixel might contain flux from multiple objects. In this case we try to first establish the shape of the stellar image, or Point Spread Function (PSF) from a bright, isolated star. The flux in an object of interest is then determined by fitting the image data to a model of the PSF. (discussed later)

4.3 Filters

Filters are used to determine the wavelength dependence for the flux measurements.

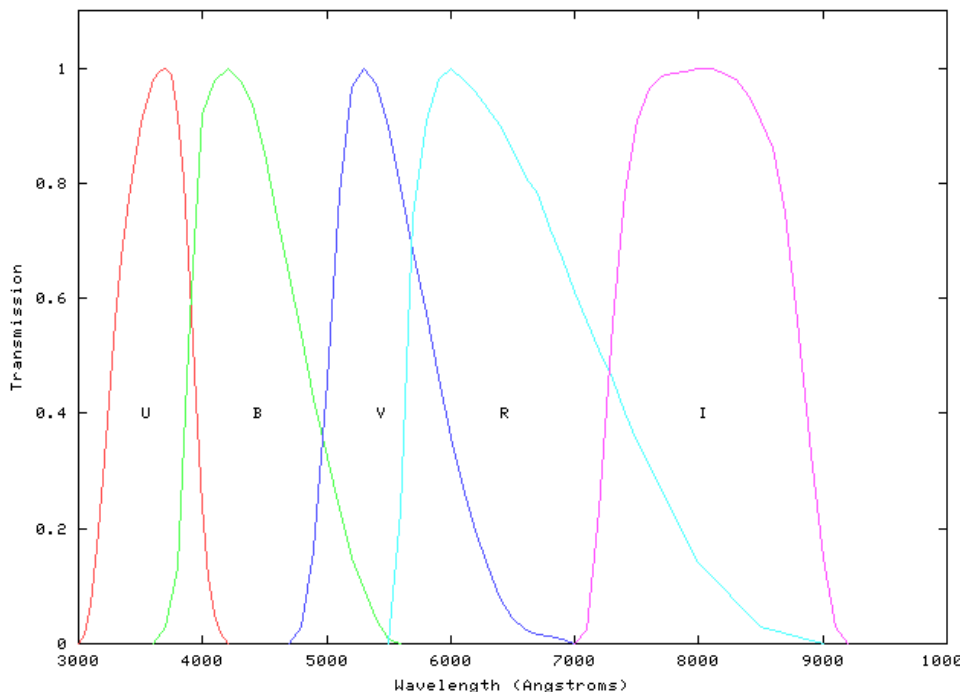


Figure 4.5 The Johnson-Cousin filter system wavelength response

One widely used filter system in the optical region of the spectrum is called the Johnson-Cousin system.

The letters correspond to different filters: U for ultraviolet, B for blue, V for visual, R for Red and I for Infrared. The central wavelengths of the filters are roughly: U – 3600 Å, B - 4400 Å, V -5500 Å, R- 6400 Å, I- 7500 Å. The wavelength range (passband) passed by each filter, is roughly 1000 Å.

We define magnitudes in each filter by V or m_V where V is the filter.

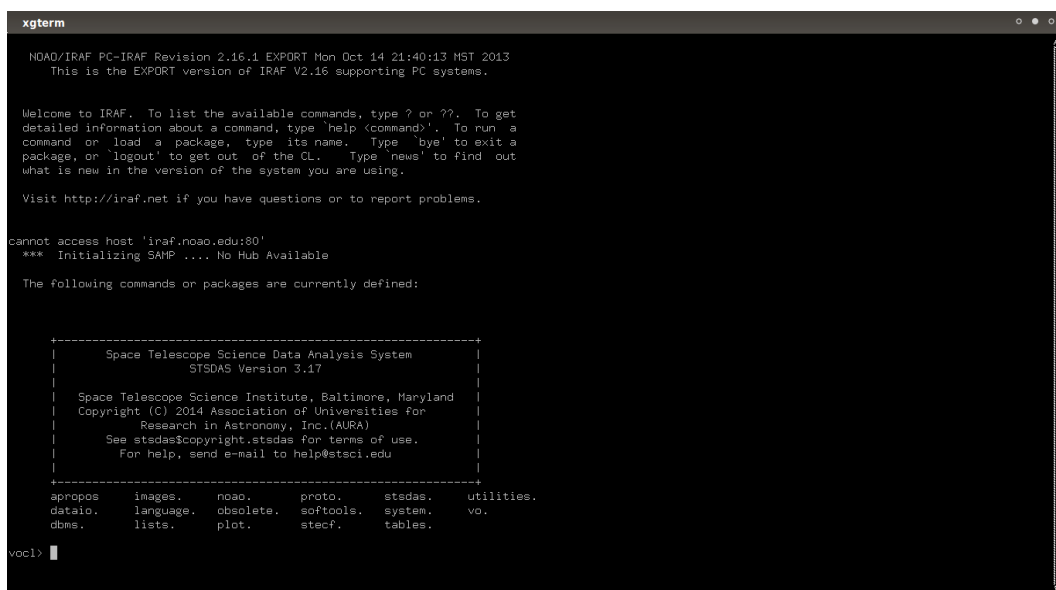
Hence, the color index as the difference between the magnitudes in filters B and V is;

$$B - V = (\text{magnitude in B filter}) - (\text{magnitude in V filter})$$

4.4 IRAF

IRAF (image reduction and analysis facility) is a collection of software written at the National Optical Astronomy Observatory (NOAO) created to perform photometry primarily from data taken from imaging array detectors such as CCDs. It is mostly used on Linux distributions. IRAF is a combination of C and FORTRAN. IRAF commands (known as tasks) are organized into package structures. Additional packages may be added to IRAF [18].

All the computational procedures in this research was done with IRAF. Refer Appendix for the coding.



```
xterm
NOAO/IRAF PC-IRAF Revision 2.16.1 EXPORT Mon Oct 14 21:40:13 MST 2013
This is the EXPORT version of IRAF V2.16 supporting PC systems.

Welcome to IRAF. To list the available commands, type ? or ?? . To get
detailed information about a command, type 'help <command>'. To run a
command or load a package, type its name. Type 'bye' to exit a
package, or 'logout' to get out of the CL. Type 'news' to find out
what is new in the version of the system you are using.

Visit http://iraf.net if you have questions or to report problems.

cannot access host 'iraf.noao.edu:80'
*** Initializing SAHP .... No Hub Available

The following commands or packages are currently defined:

-----
|           Space Telescope Science Data Analysis System           |
|           STSDAS Version 3.17                                   |
|           |                                                     |
|           Space Telescope Science Institute, Baltimore, Maryland |
|           Copyright (C) 2014 Association of Universities for    |
|           Research in Astronomy, Inc.(AURA)                    |
|           See stsdas$copyright.stsdas for terms of use.         |
|           For help, send e-mail to help@stsci.edu               |
|           |                                                     |
|-----|-----|-----|-----|-----|-----|
| apropos  images.  noao.    proto.  stsdas.  utilities. |
| datsio.  language. obsolete. softools. system.  vo.      |
| dbms.    lists.    plot.    stecf.  tables.   |
|-----|-----|-----|-----|-----|-----|

voc1> |
```

Figure 4.6 The IRAF system

CHAPTER 05

OBSERVATIONAL DATA

The telescopic data used in this research was acquired at the Mount Abu Observatory, Girishikar, Rajasthan, India. The observatory is located at 24.65 N latitude, 72.78 E longitude and has an altitude of 1680 m ^[10]. The telescope is an equatorially mounted open truss and fork type Cassegrain and has a 1.2 m parabolic primary (f/3) and a 300 mm hyperbolic secondary. A HAWAII-1 1kx1k liquid nitrogen cooled HgCdTe CCD detector array is coupled to the telescope along with a Johnson-Cousin filter system. Observations were done in the B,V filters. A large collection of frames were obtained and combined to increase the S/N ratio of the data.

Characteristics of the CCD

- Pixel Size = 18.5 μm
- Detection range (λ) = 0.85 - 2.50 μm
- Quantum Efficiency at 77K, 2 μm is 65%
- Dark current (at 77 K) < 1.0 e /s
- Read Noise = 15-20 e
- Full Well Capacity = 1.3×10^5 e
- Electron Gain = 4 e/ADU
- Field of view= 8 x 8 sq. arcmin

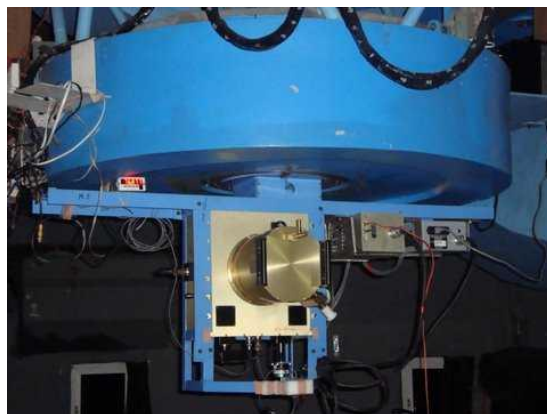


Figure 5.1 The HAWAII-1 1kx1k CCD detector

The observational data used in this research

Table 5.1

The table containing observational data

Frame	Filter	No. of frames	Exposure Time (s)
Bias	-	8	0
Flats	B	6	500
	V	12	2
Object	B	10	45
	V	10	30

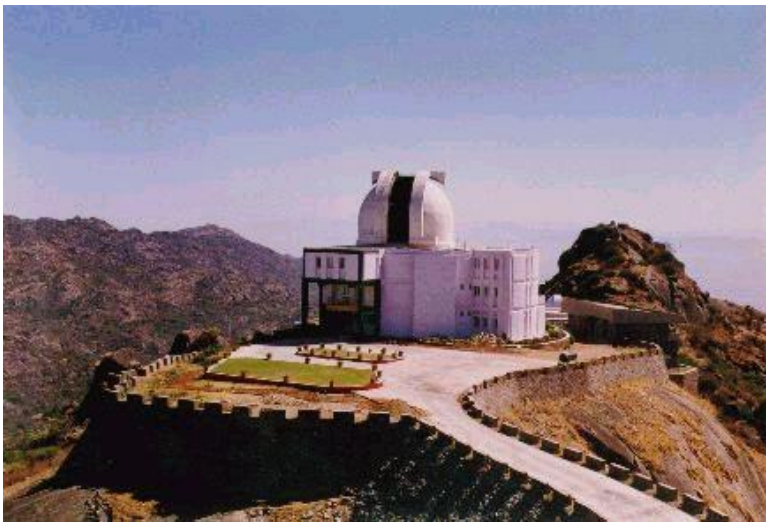


Figure 5.2 The Mount Abu Observatory and its telescope

CHAPTER 06

CCD IMAGE PROCESSING

6.1 Charged Coupled Devices

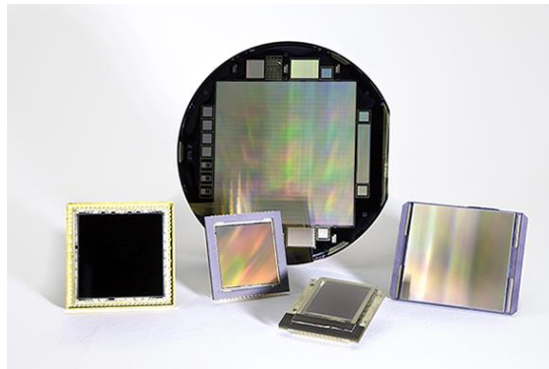


Figure 6.1 Charged Coupled Devices

A charge coupled device (CCD) is an integrated circuit etched onto a silicon surface forming light sensitive elements called pixels. Photons incident on this surface generate charge that can be read by electronics and turned into a digital representations of the light patterns falling on the device.

6.1.1 Working Principle

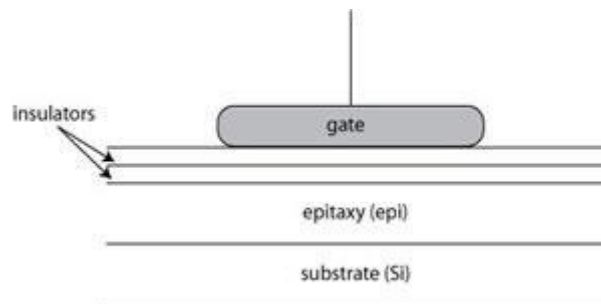


Figure 6.2 A schematic diagram of a CCD pixel

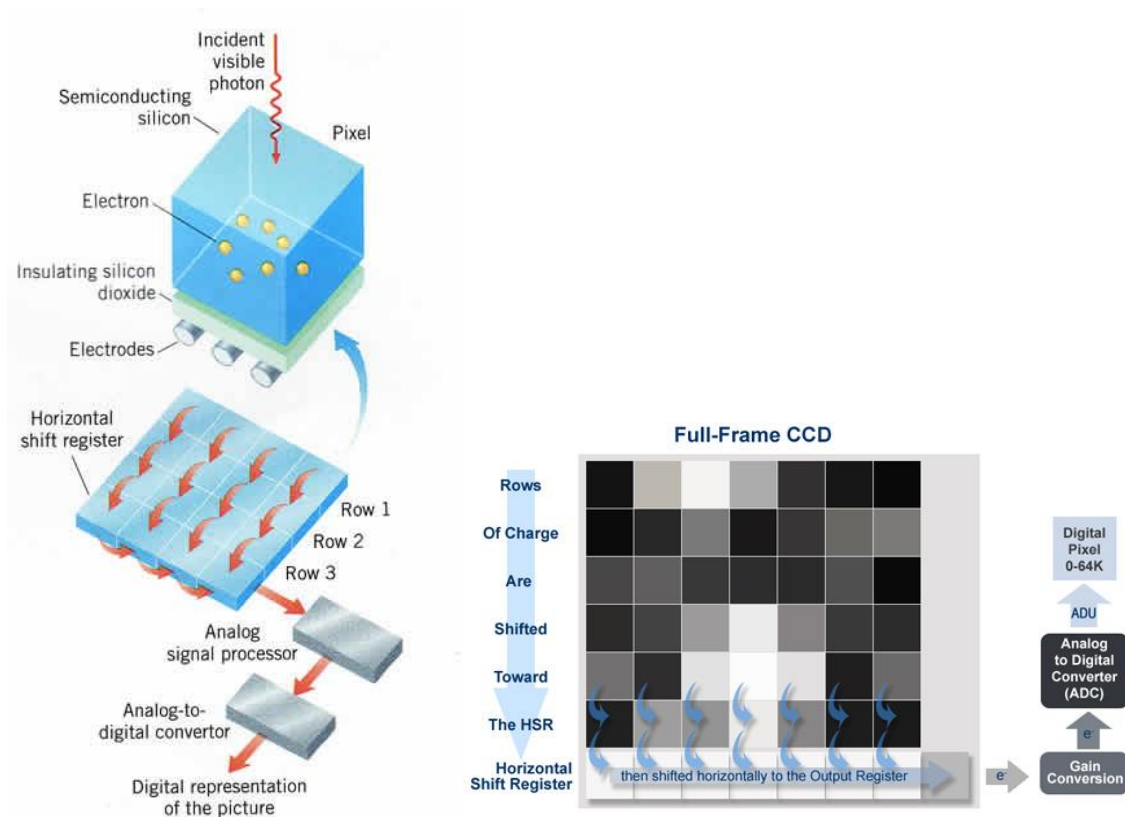


Figure 6.3 The action of a CCD

Photons striking a silicon surface create free electrons through the photoelectric effect. The gate is held at a positive charge in relation to the rest of the device, which attracts the electrons to it. Because of the insulating layer; essentially a layer of glass, the electrons cannot make it through to the gate, and are held in place by the positive charge above them.

As the voltage adjacent to the electron's pixel is brought high, they begin to migrate in this direction until the voltage in the preceding gate is then brought to zero, or low, thus effectively transferring all the electrons into its neighboring pixel.

Now that the electrons are held in place, they need to be moved to where the light signal they represent can be quantified. Electrons are shifted in two directions on a CCD, called the parallel or serial direction. One parallel shift occurs from the right to the left. The serial shift is performed from top to bottom and directs the electron packets to the output register where the electron charge is measured. This quantity is then converted to a digital value and the final output is a digital image consisting of a matrix of numbers, one per pixel, each number being related to the amount of light that falls on that pixel. (Figure 6.5)

Quantum Efficiency

All CCDs generate photoelectrons at different rates depending on the wavelength of light incident on the surface. i.e. an electron is not released for each and every photon incident on the surface. Figure 6.4 gives the Quantum Efficiency variation with the incident photon wavelength for the KAD-4200 CCD.

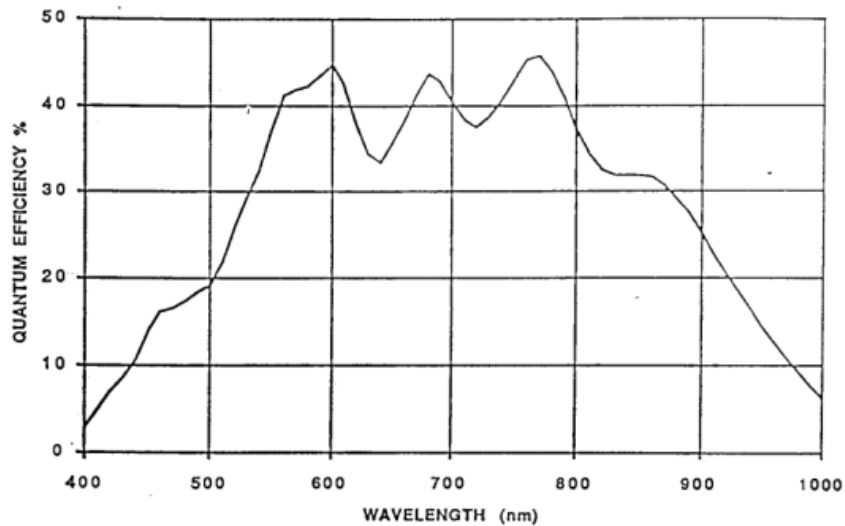


Figure 6.4 The response curve for the KAF-4200 CCD

6.2 Image Format

The pixel array matrix is saved in the FITS file format (Flexible Image Transport System).

The advantages of the FITS file are;

- The ability to perform arithmetic on the pixel values
- Contains header information related to the observations (Figure 6.6)

The values are in ADU'S (Analog to Digital Units)

$$\text{ADU} = \frac{\text{Number of Photons incident on CCD} \times \text{Quantum Efficiency of the CCD}}{\text{CCD Gain}}$$

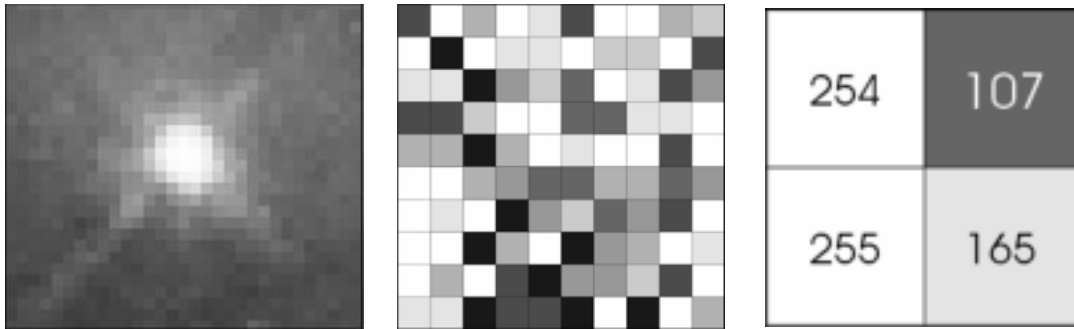


Figure 6.5 The pixel matrix of an image

```

ec1> imhead M53_V 1+
M53_V[605,569][real]:
No bad pixels, min=0., max=0. (old)
Line storage mode, physdim [605,569], length of user area 2673 s.u.
Created Sun 20:16:14 09-Nov-2014, Last modified Mon 12:30:29 10-Nov-2014
Pixel file "M53_V.fits" [ok]
EXTEND = F / File may contain extensions
ORIGIN = 'NOAO-IRAF FITS Image Kernel July 2003' / FITS file originator
DATE = '2014-11-09T14:46:14' / Date FITS file was generated
IRAF-TLM= '2014-11-10T07:00:29' / Time of last modification
COMMENT New fits header as written in fits.cpp, seqtask.cpp etc
EXPOSURE= 30 / assumed to be set in seconds
UT = 20:22:54.49 / starting time - maybe in IST
DATE-OBS= '2013-03-14T01:51:16' / starting time
OBS_END = '2013-03-14T01:51:56' / ending time
TEMP_CCD= -126.3 / temperature of CCD
TEMP_SINK= -188.7 / temperature of Sink
CCDGAIN = 4.0 / CCDGAIN
FIPOS = 4 / Filter position
PIXRATE = 1.0 / Pixel readout rate flag
COMMENT (pixrate = 0->3 : 25.3, 46.3, 104.2, 166.7 kpix/sec)
SENSITIV= 0.0 / Sensitivity flag (0->4)
COMMENT Actual value of sensitivity depends on pixel rate selected
RA = 13:13:26.36 / RA
DEC = +18:05:48.0 / DEC
GPSTIME = 20:22:54.49 / UT from GPS unit at end of observation
AIRMASS = 1.014 / airmass at which observed
COMMENT RA 13:13:26.36DEC +18:05:48.0 NTLST 12:40:58.49 UT 20:22:54.49 HRA 23:27
COMMENT 00AM 1.015 SM+120.000AZ 129.37 EL 79.997 DOM 128.9 DAY 072 G_TR
WCSDIM = 2
LTV1 = -15.
LTV2 = -1.
LTM1_1 = 1.
LTM2_2 = 1.
WAT0_001= 'system=physical'
WAT1_001= 'wtype=linear'
WAT2_001= 'wtype=linear'
IMCMB001= 'm53V01.fits'
IMCMB002= 'm53V02.fits'
IMCMB003= 'm53V06.fits'
IMCMB004= 'm53V07.fits'
NCOMBINE= 4
FILTERS = 'V'
ST = 12:40:58.49
EXPTIME = 30
UTMIDDLE= '2013-03-14T20:23:09.49'
EPOCH = 2000
  
```

Figure 6.6 The header of a FITS file

6.3 Data Reduction

Before photometric measurements of stars can be made from CCD images, it is necessary to remove artifact signals which do not represent photon counts. These include the bias level, dark signal and differences in sensitivity among pixels.

There are two types of errors in the CCD data: additive and multiplicative errors. Additive errors add to the values of pixels, multiplicative errors multiply the value in a pixel. To correct additive errors, we simply subtract a value from the image and to correct multiplicative errors, we simply divide the image by a value.

Additive errors arise from two primary sources: bias offset and dark current. There are two types of calibration images that might be used to correct these additive errors: dark and bias frames.

- Dark Frame- A dark frame is an exposure taken without any light falling on the CCD. The dark current is due to thermal excitations in the CCD. However, the CCD at Mount Abu Observatory is cryogenically cooled with liquid nitrogen, hence a dark correction is not necessary.
- Bias Frame/Zero Frame- A bias frame is a zero second exposure required to correct the bias offset. The bias offset is due to an electrical offset in the CCD.
- Flat Frame- The flat frame is an evenly illuminated field required to correct pixel sensitivity variation errors. Multiplicative errors can arise from several sources: differences in quantum efficiency, illumination differences (vignetting), and dust halos. All of these represent a difference in sensitivity from pixel to pixel in the chip, thus different pixels need to be multiplied up to larger values to match more sensitive pixels.

Other sources of errors in images include:

- Cosmic rays- Cosmic rays are high energy particles which pass through our CCD detector and deposit large amounts of energy. This deposition of energy mimics the deposition of energy by which CCD's detect photons. The ideal way to pick out cosmic rays is to take multiple images, then any bright pixels which show up in that position in only one image is a cosmic ray.

- Read noise- After an exposure, the CCD must be read out to find the signal value at each pixel. This generates a noise which is inevitable.

The **overscan region** of a CCD is provided so that each scan line has a reference to detect an offset measured at each line. This a region does not receive light, and is meant to provide information about the line-by-line bias. These columns are trimmed off the image after they are used for calibration.

6.3.1 Data Reduction Procedure

1. The bias frames were median combined into a single low noise master bias frame.
2. Flat frames were median combined into a single normalized master flat frame in each filter.
3. The master bias frame was subtracted from the Object frames (image of the celestial object). Then the object frame was divided by the master flat frame for each filter.

The procedure can be summarized as;

$$\text{Calibrated Object Frame} = \frac{\text{Raw Object Frame} - \sum \text{Bias Frame}}{\text{Normalized } (\sum \text{Flat Frame})}$$

6.4 Data Analysis

The correction frames:

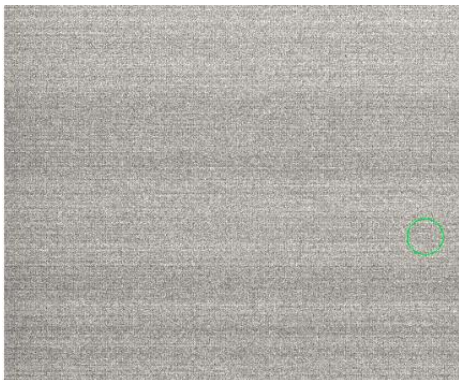


Figure 6.7 The bias frame



Figure 6.8 The flat frame

Before Reduction:

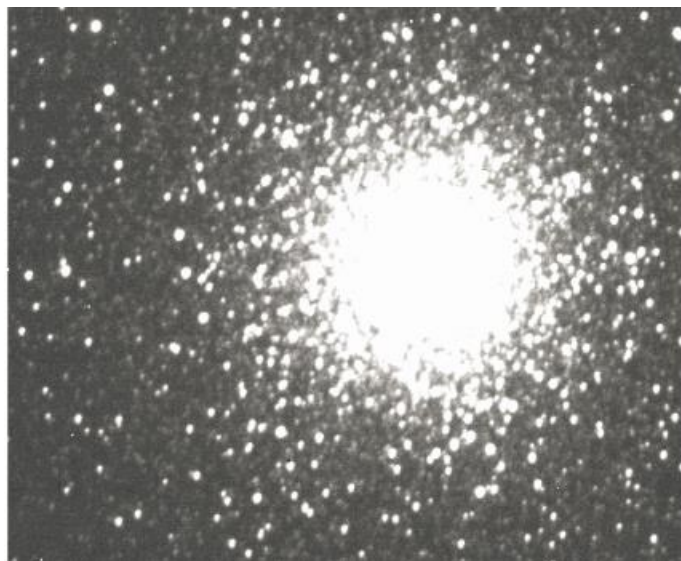


Figure 6.9 The M53 object frame in V filter before reduction

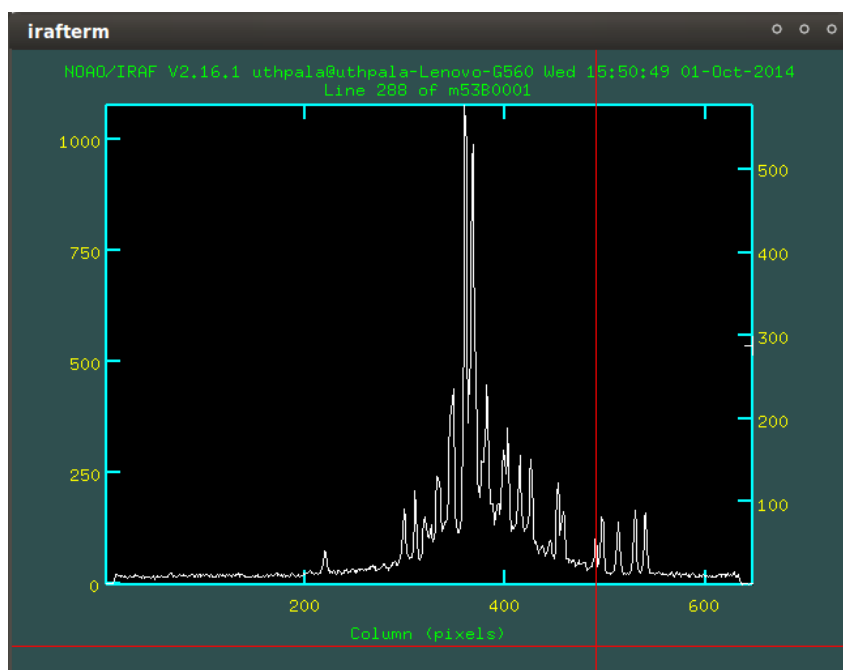


Figure 6.10 The pixel value vs. column plot for M53 in V before reduction

The overscan region was found to be [625:648,2:570] which corresponds to [x1:x2,y1:y2]. In Figure 6.10, the background contribution to the pixel value is clearly visible.

After Reduction:

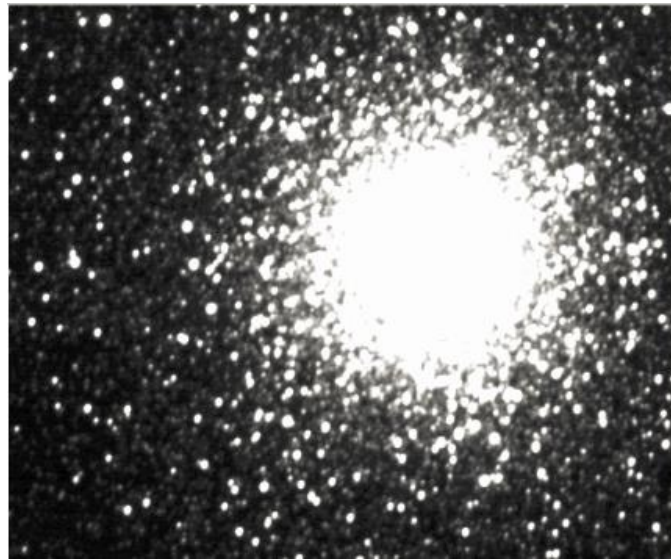


Figure 6.11 The M53 object frame in V filter after reduction

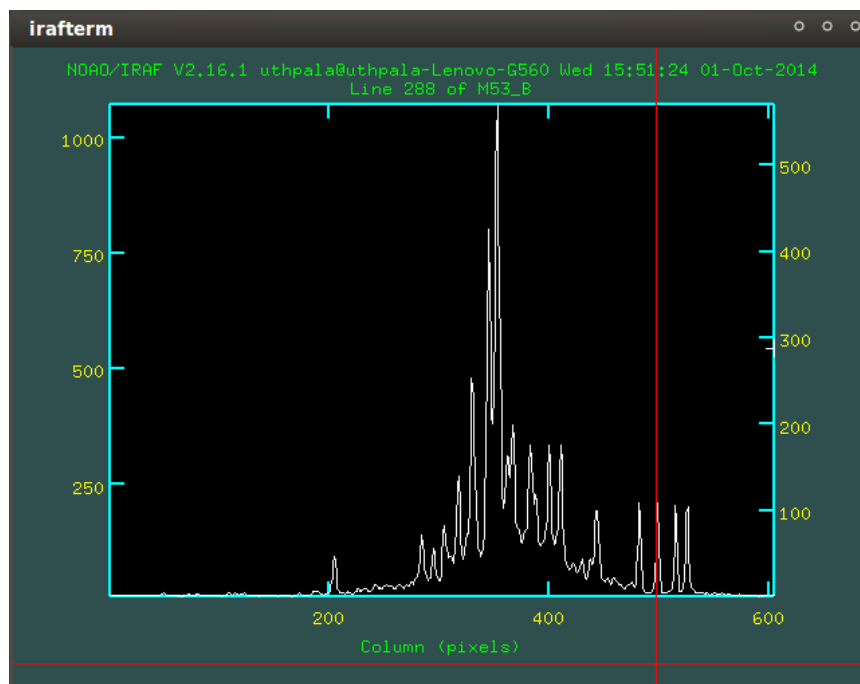


Figure 6.12 The pixel value vs. column plot for M53 in V after reduction

In figure 6.12, it can be seen that the background contribution has been completely removed. This procedure was repeated for the B frames as well. The reduced object frames are now ready for photometry. Refer appendix A for more details on the data reduction procedure.

CHAPTER 07

APERTURE PHOTOMETRY

A star is a point source, but due to the atmosphere and telescope optics, the light on a CCD is spread over a number of pixels and extends to a greater distance than it should.

To extract the magnitude of a star from the image, we must first sum the star's contribution over all pixels illuminated by it, and subtract the contribution from the sky background. We define an aperture and an annulus co-centering the star then added up all the light contribution in the aperture and subtracted the sky contribution determined from the annulus. To collect most of a stars flux, it is usually necessary to choose an aperture four to five times the size of the star. The size of a star is defined as a diameter corresponding to the Full Width Half Maximum (FWHM).^[18]

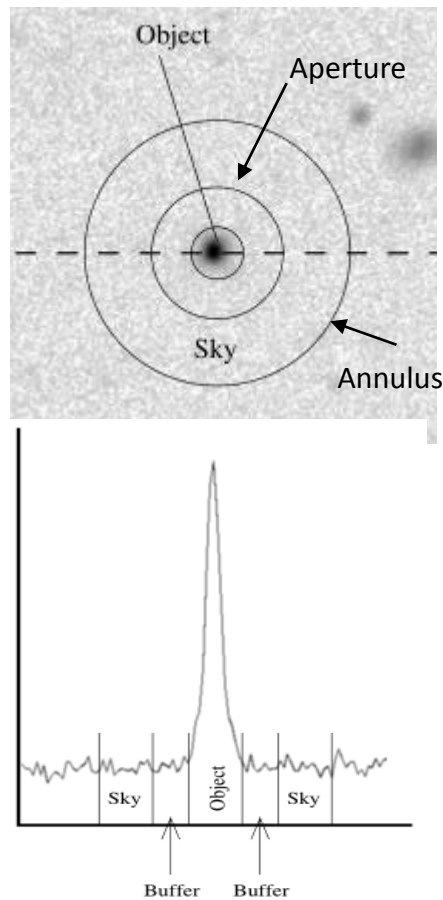


Figure 7.1 Using an aperture and annulus for aperture photometry

Measuring the starlight requires to make an aperture large enough to include all of the light from the star (use a large aperture), but aperture must be small enough that uncertainties in measuring the sky background are small (use a small aperture). The key point in aperture photometry is to determine this ideal aperture size.

To determine the required quantities, a radial profile of the star should be constructed. (Figure 7.2,7.3)

The instrumental magnitude is given by;

$$\text{Instrumental Magnitude (m)} = -2.5 \log \left(\frac{N_{ap} - A_{ap} S_{sky}}{t_{exp}} \right)$$

where,

N_{ap} - total counts in aperture

A_{ap} - area of the aperture in pixels

S_{sky} - sky signal per pixel

t_{exp} - exposure time

7.1 Data Analysis

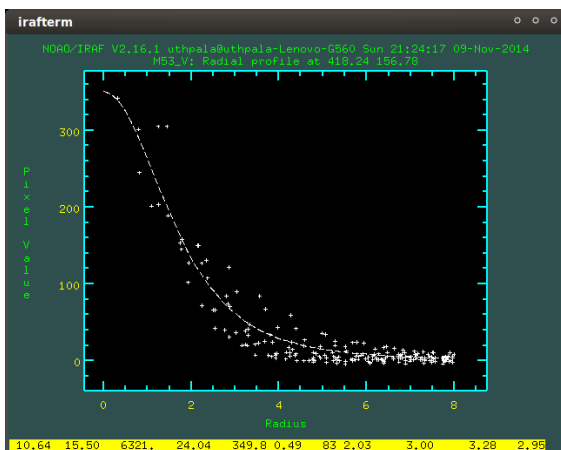


Figure 7.2 The radial plot of a V band star

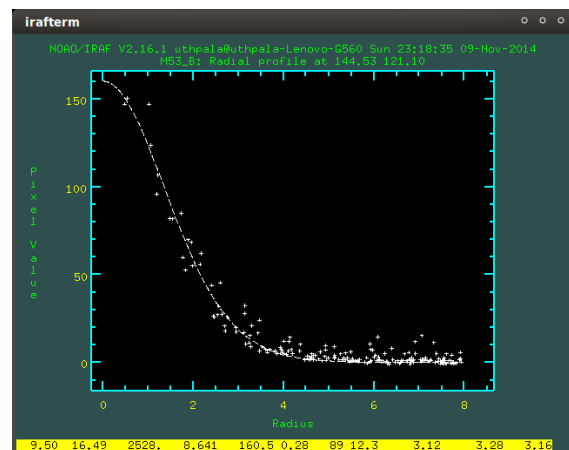


Figure 7.3 The radial plot of a B band star

Table 7.1

The average FWHM and sky values

Filter	FWHM (px)	Sky value (counts/px)
V	2.90	1.30
B	3.10	1.50

Aperture photometry was conducted for apertures of 3 px, 7px and 10px. The inner radius of the annulus was taken to be 15 px and its width 5 px.

The centering algorithm *daofind* which fits a gaussian profile to possible stars was used to locate stars in the fields.

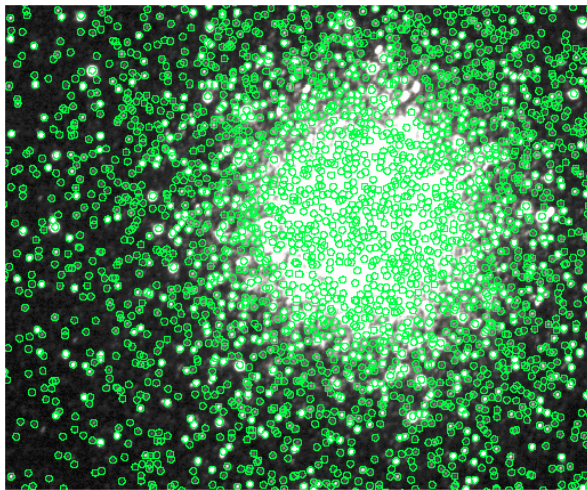


Figure 7.4 Detected stars in the V band

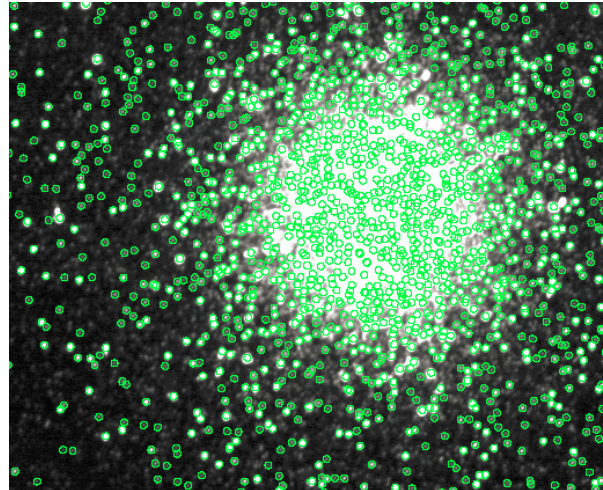


Figure 7.5 Detected stars in the B band

The extracted B and V magnitudes were then used to construct the CMD for the globular cluster.

CHAPTER 08

PSF-FITTING PHOTOMETRY

In this method, a model PSF (Figure 8.1) is constructed and is fitted to each star in the field. This is done by choosing candidate stars in the same field that are uncrowded to make an initial determination of the PSF. Next, every star in the field can be de-convolved by using methods such as a Fourier transform and the resulting flux can be measured by using a smaller aperture. These stars are then subtracted from the field leaving behind only the stars that were not initially detected. Stars that are crowded and obscured by one another in the image can be more accurately identified and measured using a smaller aperture.

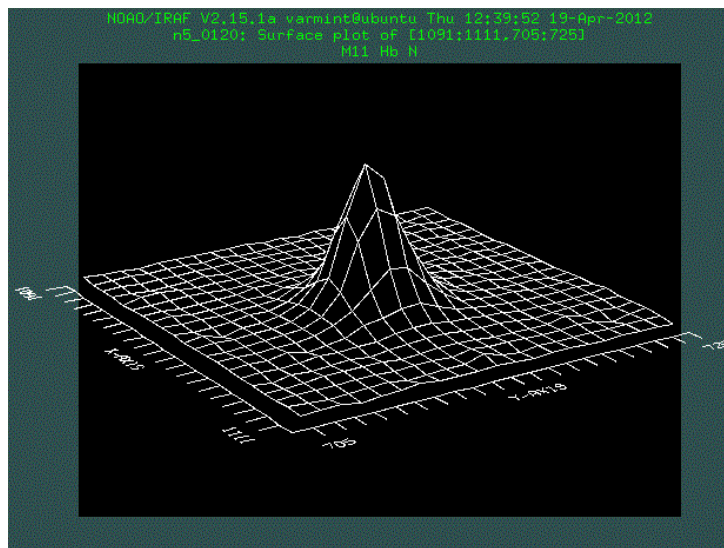


Figure 8.1 A modeled psf

PSF fitting can identify and subtract some stars even if they are crowded and almost impossible to measure by ordinary aperture methods. By doing several iterations, the flux of obscured stars can be measured.

8.1 Aperture corrections

Because a larger aperture was selected for the standard stars, the PSF data must be corrected to compensate for the use of a smaller aperture. A curve-of-growth constructed using several aperture radii is used for this purpose.

8.2 Data Analysis

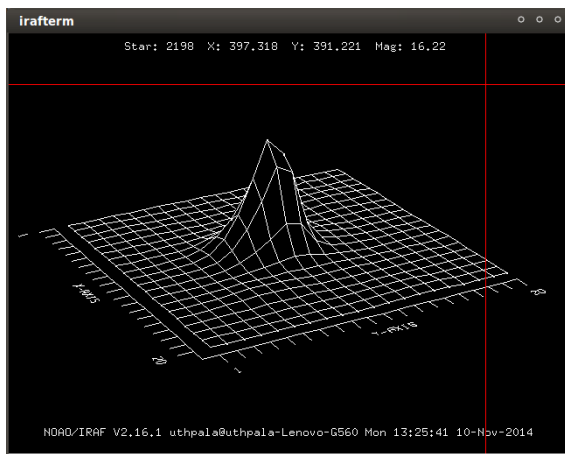


Figure 8.2 A “good” psf model

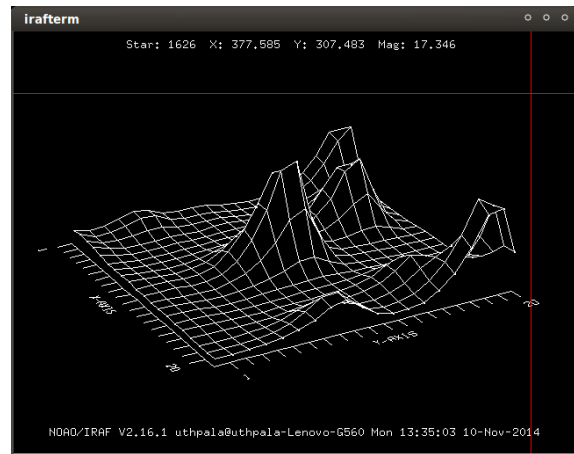


Figure 8.3 A defective psf model

The aperture sizes used were 3 px and 3.3 px for V & B filters respectively. The inner radius of the annulus was taken to be 7 px and its width 3 px.

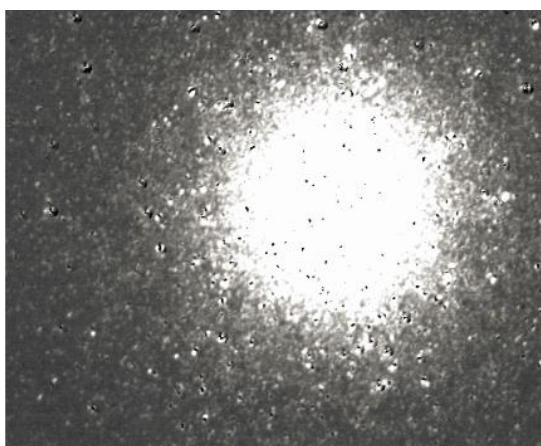


Figure 8.4 The psf subtracted V field

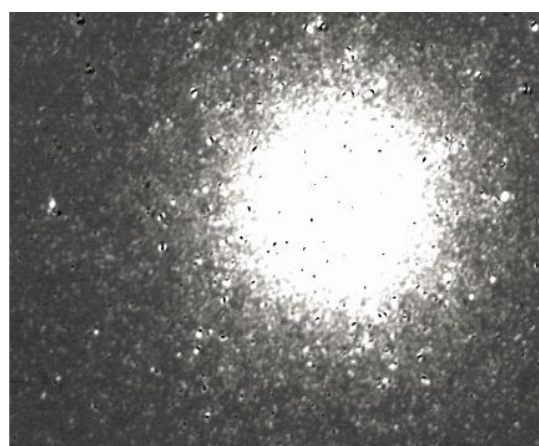


Figure 8.5 The psf subtracted B field

Aperture Correction

Aperture used for standard stars= 6 px

Aperture used for PSF- Fitting photometry=3 px (V) and 3.3 px (B)

$$\text{Aperture correction } (\Delta) = \frac{\sum(\text{mag}_{AP(3 \text{ px or } 3.3 \text{ px})} - \text{mag}_{AP(6 \text{ px})})}{n}$$

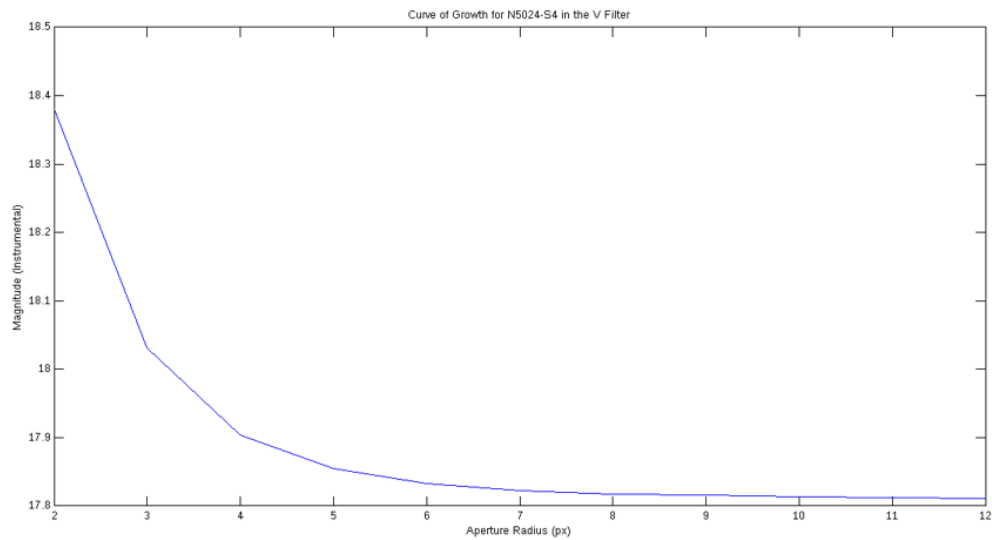


Figure 8.6 The Curve of Growth for the V band

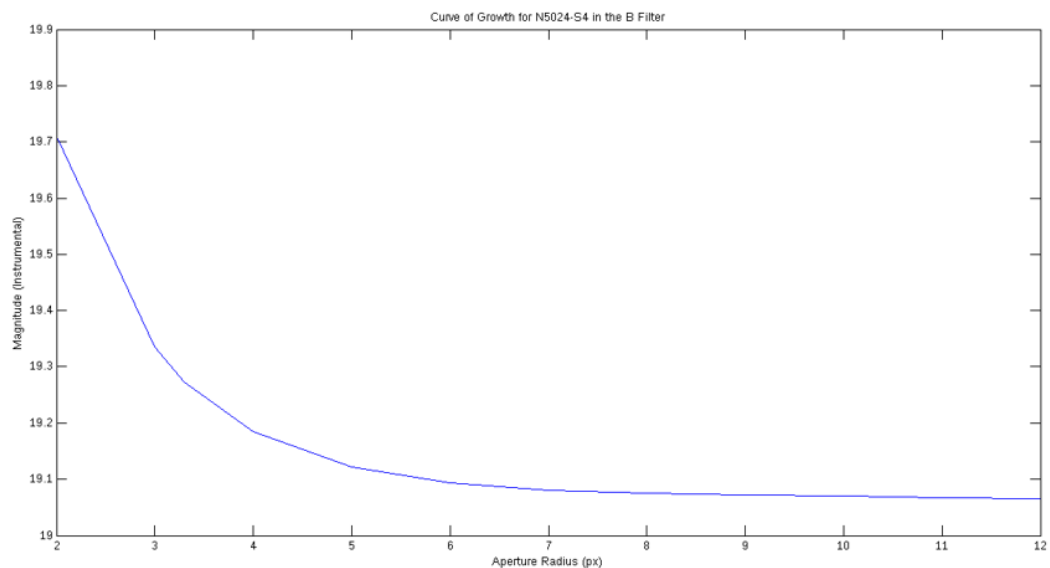


Figure 8.7 The Curve of Growth for the B band

Table 8.1

The aperture correction values

Filter	Aperture Correction (mag)
V	-0.2228589
B	-0.2036152

The extracted B and V magnitudes were then used to construct the CMD for the globular cluster.

CHAPTER 09

STANDARD MAGNITUDE CALIBRATION

9.1 Extinction and Airmass

The flux received from a star decreases due to atmospheric extinction. The calibration of the instrumental magnitudes to the standard system involves an extinction correction. The attenuation due to atmospheric extinction describes the degree to which a particular wavelength is scattered or blocked by the air. The amount of the air is called airmass, and is typically 1 for a star directly overhead. The angle between the star and the point overhead, the zenith angle ζ , determines the value of the airmass. The airmass can be approximated $X = \sec(\zeta)$ by trigonometry. (Figure 9.1) Due to curvature of atmospheric layers, for $\zeta > 60^\circ$, it becomes necessary to include higher order trigonometric terms to calculate a useful approximation of airmass. ^[17]

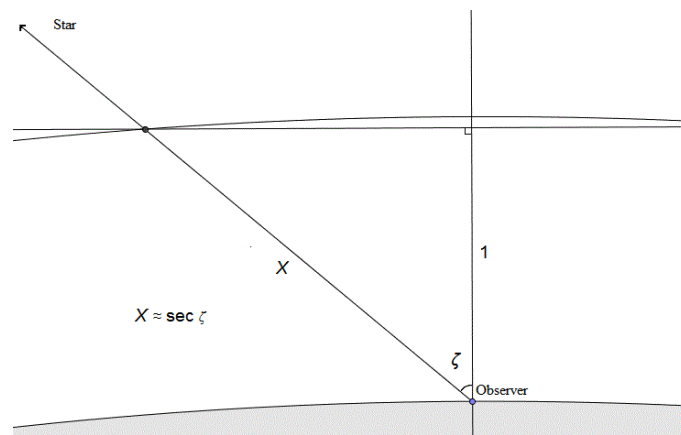


Figure 9.1 The airmass of the atmosphere

The following formula was used to calculate the airmass.

$$\text{Airmass (X)} = \sec(\zeta) = \frac{1}{[\sin\lambda\sin\delta + \cos\lambda\cos\delta\cos h]}$$

where,

λ - latitude of the observatory

δ - declination of object

h- hour angle of object at the time of observation

9.1.1 Data Analysis

Table 9.1

Airmasses calculated for the B and V filters.

Filter	Effective Airmass (X)
B	1.008
V	1.014

9.2 Transformation Equations

The magnitudes obtained from the above aperture photometry and psf-fitting photometry methods are instrumental magnitudes. i.e. they are unique to the telescope used. However, since the flux received on earth from a star must be the same for all observers, the instrumental magnitudes must be converted into standard magnitudes. Transformation equations are used for this purpose. The airmass correction and magnitudes of standard stars retrieved from a standard star catalogue are used in these equations. Once the transformation equations are obtained, all the instrumental magnitudes can be calibrated with the standard system.

9.2.1 Data Analysis

Magnitudes of 12 standard stars were obtained from the Stetson (2000) catalogue. Next, Aperture Photometry was performed on them using a 6 px aperture.

For the purpose of matching standard stars to instrumental stars astronomical the software package Aladin v8.0 was utilized.

The generic transformation equation is given by;

$$m=M + z_0+ KX$$

where,

M- standard magnitude

m- instrumental magnitude

z_0 - zero point constant

K- atmospheric absorption co-efficient

X- airmass

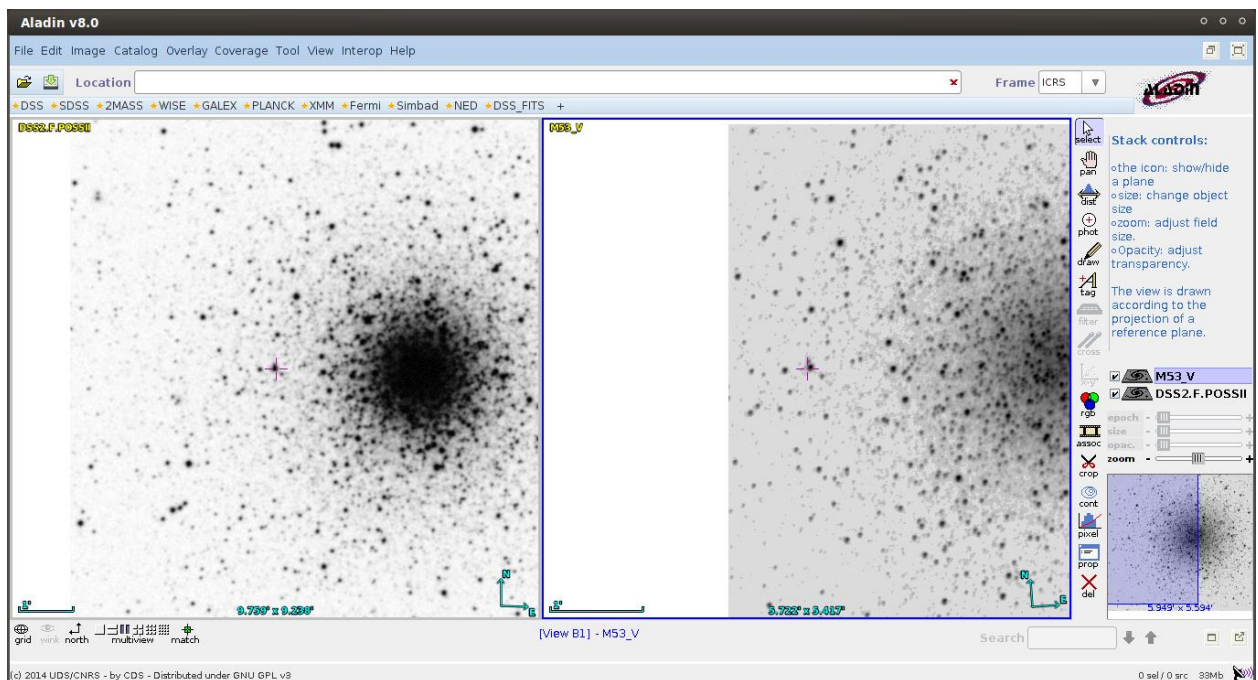


Figure 9.2 Aladin standard star locator

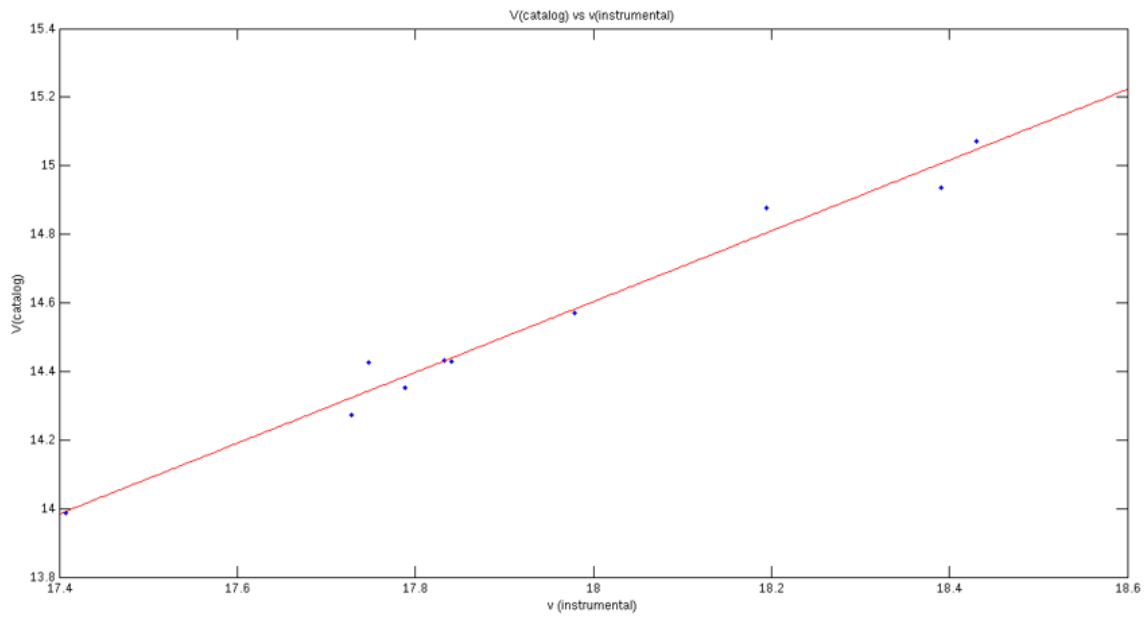


Figure 9.3 The graph of V (catalog) vs v (instrumental)

Transformation equation for the V filter $\rightarrow V=v-3.97$

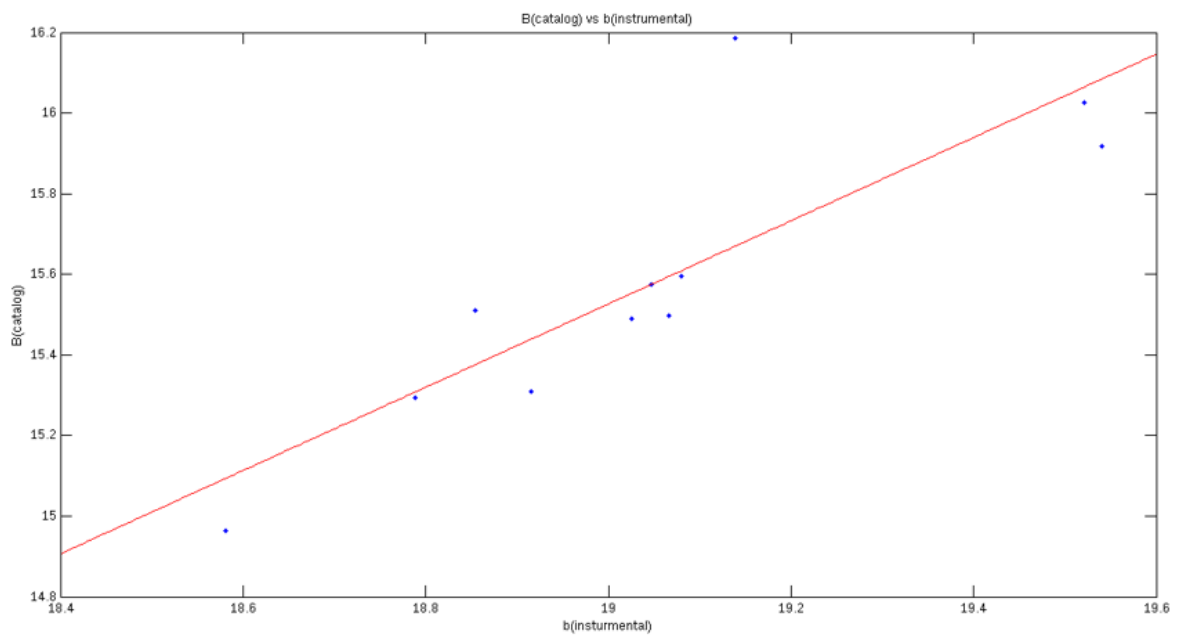


Figure 9.4 The graph of B (catalog) vs b (instrumental)

Transformation equation for the B filter $\rightarrow B=b-4.09$

CHAPTER 10

UNCERTAINTIES

All scientific measurements carry an uncertainty or error in a measurement. In photometry, the uncertainty is due to noise. The signal/noise is given by;

$$S/N = \frac{R_* \times t}{[(R_* \times t) + (R_{sky} \times t \times n_{pix}) + (RN^2 + (\frac{G}{2})^2 \times n_{pix}) + (D \times n_{pix} \times t)]^{1/2}}$$

where,

R_* - count rate from star (e/s)

R - sky count rate from background (e/s/pix)

t - exposure time (s)

r - radius of aperture (px)

n_{pix} - number of pixels in aperture (πr^2)

G - gain (e/DN)

D - dark current (e/s/px)

$$\text{Uncertainty in magnitude } \sigma(m) = \pm 2.5 \log\left(1 + \frac{1}{S/N}\right)$$

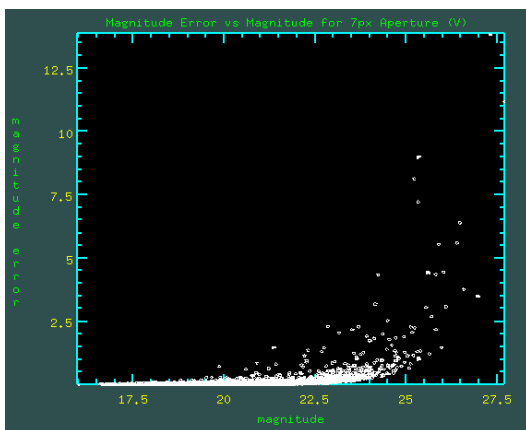


Figure 10.1 Aperture photometry mag error

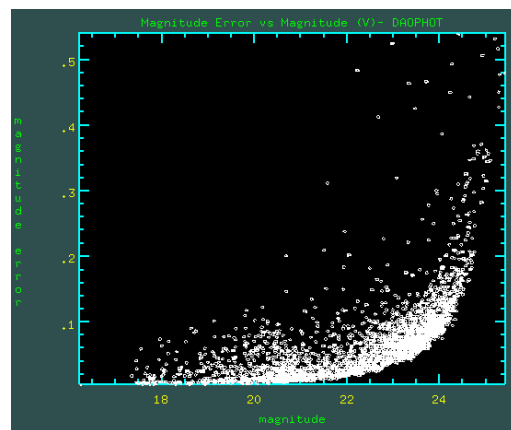


Figure 10.2 PSF photometry mag error

CHAPTER 11

RESULTS AND ANALYSIS

11.1 Aperture Photometry Results

11.1.1 Aperture Radius= 10 px

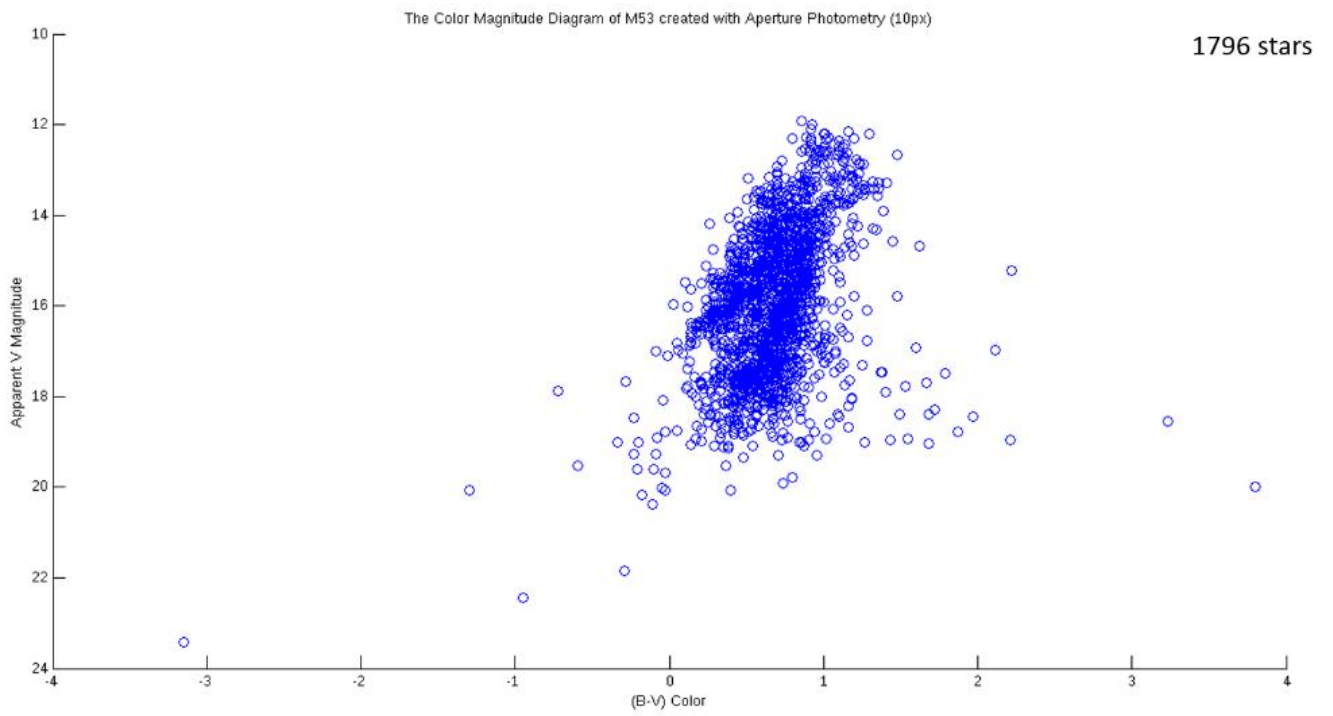


Figure 11.1 The CMD of M53 for 10px aperture

11.1.2 Aperture Radius= 7 px

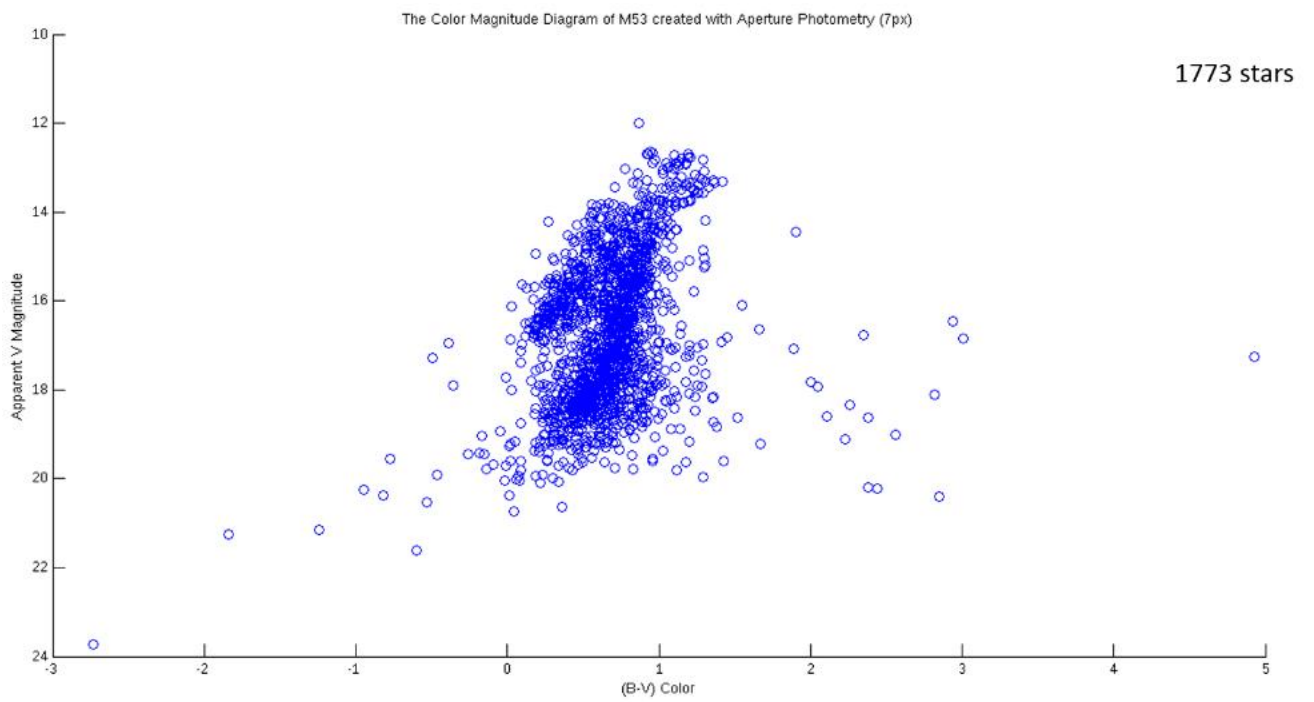


Figure 11.2 The CMD of M53 for 7px aperture

11.1.3 Aperture Radius= 3 px

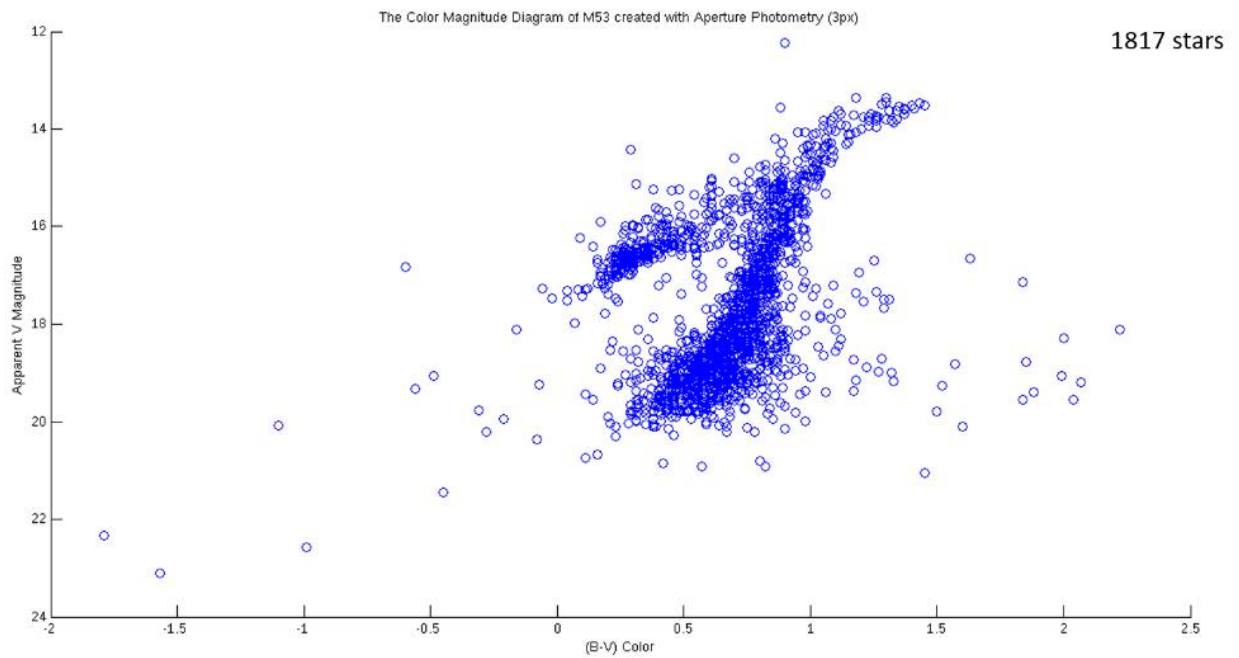


Figure 11.3 The CMD of M53 for 3px aperture

11.2 PSF- Fitting Photometry Results

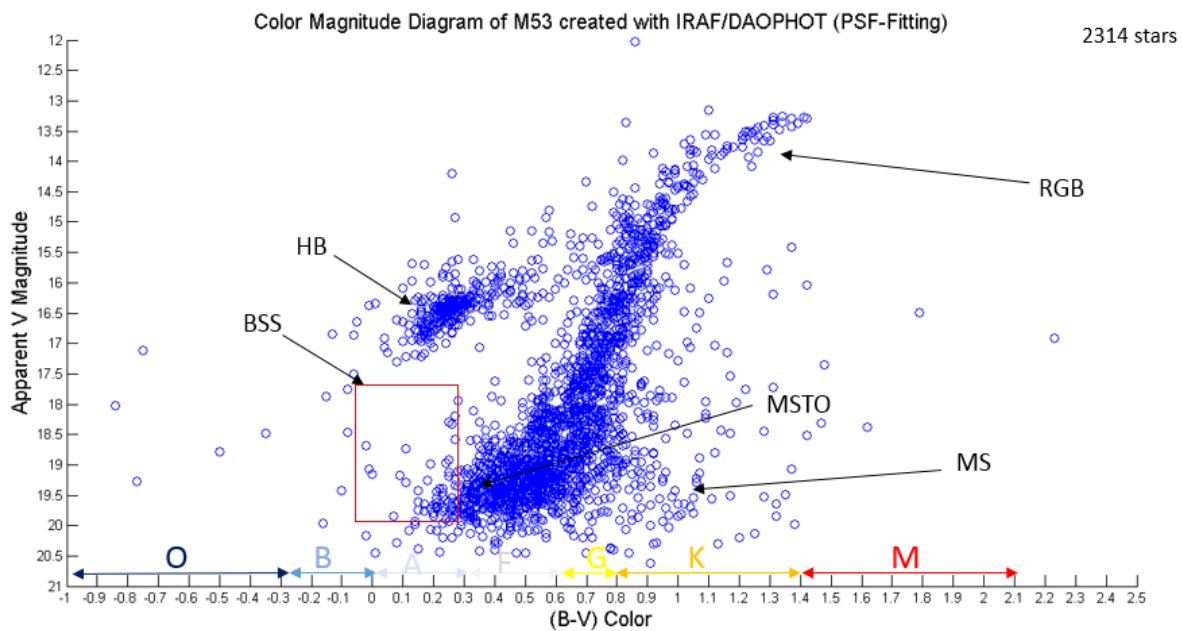


Figure 11.4 The CMD of M53 using PSF-Fitting photometry

11.3 Analysis

CMD's obtained from apertures 7 px (Figure 11.2) and 10 px (Figure 11.1) convey no useful information whatsoever. CMD obtained from 3 px (Figure 11.3) aperture shows a distinguishable Horizontal Branch and a small portion of the Red Giant Branch but the Main Sequence Turn off point cannot be determined.

Hence, it can be said that Aperture Photometry is not ideal for crowded fields. This is probably because the apertures were contaminated with neighboring stars, hence giving over-exceeded flux values.

However, the CMD (Figure 11.4) obtained from PSF-Fitting photometry using 2314 stars conveys quite a lot of information about the globular cluster since almost all regions are present.

From figure 11.4, the Main Sequence Turn Off point is $(V_{TO}) = 18.43 \pm 0.06$ and $(B - V)_{TO} = 0.449 \pm 0.064$. This $(B - V)$ value corresponds to a F5 type star which has an absolute magnitude $(M_v) +3.9$ [16]. Hence, the distance modulus $(m - M_v)$ was calculated to be 14.53 ± 0.23 .

The relationship between the distance modulus and the distance (d) to the cluster is given by;

$$d = 10^{\frac{(m-M)+5}{5}} \text{ pc}$$

Hence, the distance to the cluster was found to be 8.05 kpc.

Since, the F5 type star resides in the MSTO point of the CMD, taking the lifetime of a F5 type star into account, it can be said that the cluster is atleast 3.2 Gyr old. It is also safe to say that O and B type stars have left the main sequence. Also, 19 Blue Straggler stars were found within the region $0 < (B-V) < 0.3$ and $17 < V < 19$

Table 11.1

Summary of obtained values

Property	Value	Previous research	Source
Main Sequence Turn off point	$(B - V)_{TO} = 0.449 \pm 0.064$ $V_{TO} = 18.43 \pm 0.06$	$(B - V)_{TO} = 0.403 \pm 0.001$ $V_{TO} = 20.30 \pm 0.04$	[14]
Distance Modulus ($m - M_v$)	14.53 ± 0.23	16.28	[13]
Distance to cluster	8.05 kpc	18.2 kpc	[13]
Approximate age estimate of the cluster	atleast 3.2 Gyr	12 Gyr	[15]

11.4 Conclusion

It was clearly noted that the aperture photometry method fails for crowded fields like globular clusters. For smaller aperture sizes, the Horizontal Branch and a portion of the Red Giant Branch appears vaguely. The PSF- Fitting photometry method yields a much better CMD with a distinguishable Horizontal Branch, a Red Giant Branch, a Main Sequence and a Blue Straggler region. The research results for MSTO points and the distance modulus is in fair agreement with previous research results. However, there seems to be a significant deviation in the distance and age of the globular cluster. For the latter, this may have been due to the fact that only a rough estimate was obtained for the age. Employing isochrones fitting methods would yield a far accurate result. A distinguishable Blue Straggler Star population was seen to exist in the globular cluster M53.

REFERENCES

- [1] E. Eva, *Globular clusters and open clusters difference*, Retrieved 28th June, 2014 from <http://www.sciences360.com/index.php/globular-clusters-and-open-clusters-difference-6818/>
- [2] R. Jimenez, *Proc Natl Acad Sci:USA* 95 (1998)
- [3] M. Richmond, *Interpreting the HR diagrams of stellar clusters*, Retrieved 14th June, 2014 from <http://spiff.rit.edu/classes/phys230/lectures/clusters/clusters.html>
- [4] J. Gross, *RoanokeValley Astronomical Society* 28-5 (2011)
- [5] M. Drout, *A second case for a double Blue Straggler sequence*, Retrieved 25th June, 2014 from <http://astrobites.org/2013/10/21/a-second-case-for-a-double-blue-straggler-sequence/>
- [6] T. Plotner, *Messier 53*, Retrieved 14th June, 2014 from <http://www.universetoday.com/36025/messier-53/>
- [7] E. Budding, O. Demircan, *Introduction to Astronomical Photometry (2nd edition)*, Cambridge University Press (2007)
- [8] A. Sandage, *Astron J* 58:51-75 (1953)
- [9] E. Dalessandro, F. R. Ferraro, D. Massari et al., *Double Blue Straggler sequences in GCs: the case of NGC 362*, University of Bologna Department of Physics and Astronomy (2013)
- [10] R. R. Shah et al, *Bull. Astr. Soc. India* (2005) 33, 237{243
- [11] Raymond E. White, *ApJs* 19.343W (1970)
- [12] James Cuffey, *ApJ* 128.219C (1958)
- [13] Heasley J.N., Christian C.A., *AJ* 101.967H (1991)
- [14] Soo-Chang Rey et al, *Astron J* 116:1775-1788 (1998)
- [15] Young-Beom Jeon et al, *Astron J* 125:3165-3174 (2003)
- [16] Binney, J. Merrifield, M., (1993), *Galactic Astronomy*, Princeton University Press
- [17] Romanishin W., *An introduction to Astronomical Photometry Using CCD's*, University of Oklahoma (2006)
- [18] Massey P., Davis L., *A User's guide to Stellar CCD Photometry with IRAF*, Retrieved from <http://iraf.noao.edu/docs/docmain.html>

APPENDIX A

A.1 M53 Data Reduction Procedure

01. The bias frames were combined into a single bias file, **bias.fits**.

```
cl>imcombine @bias_list bias combine=median
```

@bias_list contains all the bias files.

02. The bias was subtracted from all the frames.

```
cl>imarith @flat_b_list - bias @flat_b_list
```

```
cl>imarith @object_b_list - bias @object_b_list
```

@flat_b_list contains the flats for the B filter.

@object_b_list contains the object frames for the B filter.

This was repeated for flats and object frames the V filter.

03. The flats were combined.

Image statistics were examined to remove significantly different frames.

```
cl>imstat @flat_b_list
```

#	IMAGE	NPIX	MEAN	STDDEV	MIN	MAX
	FlatsB0001.fit	373248	-11680.	3506.	-31404.	31079.
	FlatsB0002.fit	373248	10862.	2052.	6.	12329.
	FlatsB0003.fit	373248	10243.	1935.	7.	11651.
	FlatsB0004.fit	373248	9668.	1827.	7.	11106.
	FlatsB0005.fit	373248	9062.	1720.	6.5	10359.
	FlatsB0006.fit	373248	8568.	1624.	5.	9799.

Figure A.1 Image statistics for flat files in B filter

As seen in Figure A.1, the mean of the image FlatsB0001.fit is highly deviated from the rest. Hence it was removed.

Then, the remaining frames were combined into a single flat frame, **flat_B.fits**.

```
cl>imcombine @flat_b_list flat_B combine=median scale=mode
```

This procedure was repeated for the V flat frame => **flat_V.fits**.

04. BIASSEC & TRIMSEC Corrections

The flat frames were plotted to determine the trimsec and biassec (overscan) regions.

```
cl>implot FlatsV0001
```

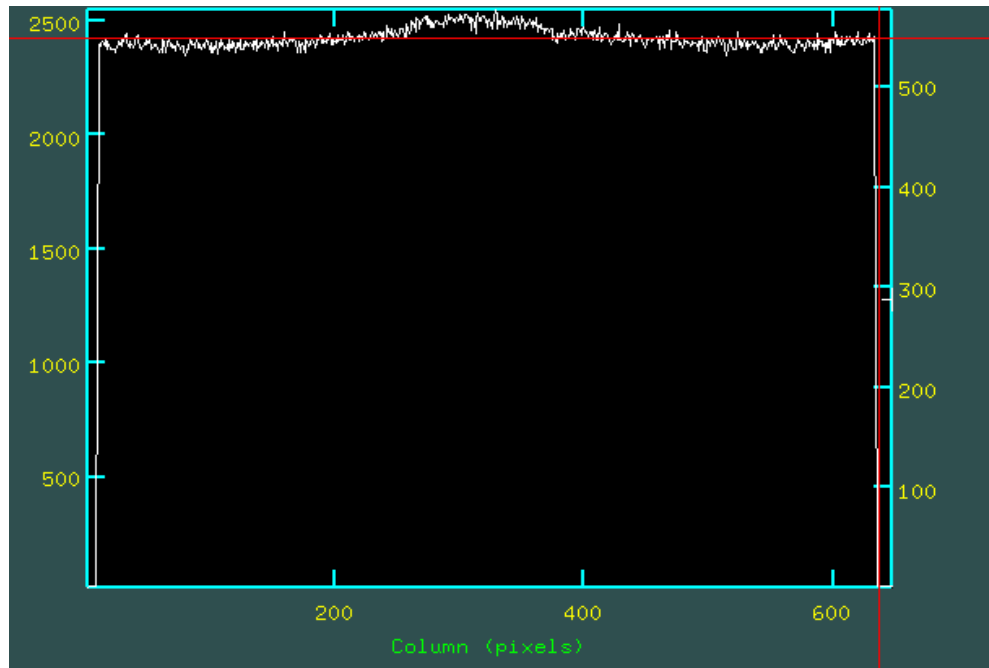


Figure A.2 implot of FlatV0001 used to determine trimsec and biassec regions

Results obtained:

```
BIASSEC=[625:648,2:570]
```

```
TRIMSEC=[16:620,2:570]
```

The correction was applied to all the frames (B, V flat & object frames)

```
cl>colbias *.fits *.fits bias=[625:648,2:570] trim=[16:620,2:570]
```

05. The flat frames were normalized.

The image statistics of the flats were viewed to obtain their modes.

```
cl>imstat flat fields="image,mode"
```

```

vocl> imstat flat_B,flat_R,flat_V fields="image,mode"
#          IMAGE      MODE
          flat_B      6357.
          flat_R      1340.
          flat_V      2444.

```

Figure A.3 image statistics of the flat frames

Then each flat frame was divided by their respective mode.

```

cl>imarith flat_B / 6357 flat_B_norm
cl>imarith flat_V / 2444 flat_V_norm

```

06. Normalizing object frames

All the object frames were divided by their corresponding normalized flat.

```

cl>imarith @object_b_list / flat_B_norm @object_b_list_n
cl>imarith @object_V_list / flat_V_norm @object_V_list_n

```

@object_b_list_n contains files in the form, **n_m53B0001.fit**

07. The object frames were aligned.

A reference frame (say **n_m53B0001**) and the frame which requires aligning (say **n_m53B0002**) were viewed in ds9. Using the command **imexamine**, the relative shift of the second frame from the reference frame was calculated.

Then the frames were aligned using **imshift**.

```

cl>imshift n_m53B0002 m53B02 xshift=-0.46 yshift=0.22

```

This was repeated for all the object frames for each filter type.

08. The aligned object frames were then combined.

```
cl>imcombine m53B*.fits M53_B combine=median reject=crreject  
cl>imcombine m53V*.fits M53_V combine=median reject=crreject
```

This resulted in three object frames for B & V filters. =>

M53_B.fits

M53_V.fits

APPENDIX B

B.1 IRAF commands for aperture photometry

Location: noao/digiphot/apphot

B.1.1 V filter

```
ap> lpar datapars
    (scale = 1.)           Image scale in units per pixel
    (fwhmpsf = 2.9)       FWHM of the PSF in scale units
    (emission = yes)      Features are positive ?
    (sigma = 1.3)         Standard deviation of background in
counts
    (datamin = 0.)        Minimum good data value
    (datamax = INDEF)     Maximum good data value
    (noise = "poisson")   Noise model
    (ccdread = "")        CCD readout noise image header keyword
    (gain = "")           CCD gain image header keyword
    (readnoise = 15)      CCD readout noise in electrons
    (epadu = 4)           Gain in electrons per count
    (exposure = "")       Exposure time image header keyword
    (airmass = "")        Airmass image header keyword
    (filter = "")         Filter image header keyword
    (obstime = "")        Time of observation image header
keyword
    (itime = 1.)          Exposure time
    (xairmass = INDEF)    Airmass
    (ifilter = "INDEF")   Filter
    (otime = "INDEF")     Time of observation
    (mode = "ql")

ap> lpar centerpars
    (calgorithm = "centroid") Centering algorithm
    (cbox = 5.)           Centering box width in scale units
    (cthreshold = 0.)     Centering threshold in sigma above
background
    (minsnratio = 1.)     Minimum signal-to-noise ratio for
centering
    (cmaxiter = 10)       Maximum number of iterations for
centering
    (maxshift = 1.)       Maximum center shift in scale units
    (clean = no)           Symmetry clean before centering ?
    (rclean = 1.)         Cleaning radius in scale units
    (rclip = 2.)          Clipping radius in scale units
    (kclean = 3.)         Rejection limit in sigma
    (mkcenter = no)       Mark the computed center on display ?
    (mode = "ql")

ap> lpar photpars
    (weighting = "constant") Photometric weighting scheme for wphot
```

```

    (apertures = "2,3,4,5,7,9,10,12,15") List of aperture radii in scale
unit
    (zmag = 25.)           Zero point of magnitude scale
    (mkapert = no)        Draw apertures on the display
    (mode = "ql")

```

```

ap> lpar fitskypars
    (salgorithm = "centroid") Sky fitting algorithm
    (annulus = 15.)         Inner radius of sky annulus in scale
units
    (dannulus = 5.)       Width of sky annulus in scale units
    (smooth = no)         Boxcar smooth the histogram
    (rgrow = 0.)          Region growing radius in scale units
    (mksky = no)          Mark sky annuli on the display
    (mode = "ql")

```

B.1.2 B filter

```

ap> lpar datapars
    (scale = 1.)           Image scale in units per pixel
    (fwhmpsf = 3.1)       FWHM of the PSF in scale units
    (emission = yes)      Features are positive ?
    (sigma = 1.5)         Standard deviation of background in
counts
    (datamin = 0.)        Minimum good data value
    (datamax = INDEF)     Maximum good data value
    (noise = "poisson")   Noise model
    (ccdread = "")        CCD readout noise image header keyword
    (gain = "")           CCD gain image header keyword
    (readnoise = 15)      CCD readout noise in electrons
    (epadu = 4)           Gain in electrons per count
    (exposure = "")       Exposure time image header keyword
    (airmass = "")        Airmass image header keyword
    (filter = "")         Filter image header keyword
    (obstime = "")        Time of observation image header
keyword
    (itime = 1.)          Exposure time
    (xairmass = INDEF)    Airmass
    (ifilter = "INDEF")   Filter
    (otime = "INDEF")     Time of observation
    (mode = "ql")

```

```

ap> lpar centerpars
    (calgorithm = "centroid") Centering algorithm
    (cbox = 5.)           Centering box width in scale units
    (cthreshold = 0.)     Centering threshold in sigma above
background
    (minsnratio = 1.)     Minimum signal-to-noise ratio for
centering
    (cmaxiter = 10)       Maximum number of iterations for
centering
    (maxshift = 1.)       Maximum center shift in scale units
    (clean = no)          Symmetry clean before centering ?
    (rclean = 1.)         Cleaning radius in scale units
    (rclip = 2.)          Clipping radius in scale units
    (kclean = 3.)         Rejection limit in sigma
    (mkcenter = no)       Mark the computed center on display ?

```

```

        (mode = "ql")

ap> lpar photpars
  (weighting = "constant")      Photometric weighting scheme for wphot
  (apertures = "2,3,4,5,7,9,10,12,15") List of aperture radii in scale
unit
  (zmag = 25.)                 Zero point of magnitude scale
  (mkapert = no)               Draw apertures on the display
  (mode = "ql")

ap> lpar fitskypars
  (salgorithm = "centroid")     Sky fitting algorithm
  (annulus = 15.)              Inner radius of sky annulus in scale
units
  (dannulus = 5.)             Width of sky annulus in scale units
  (smooth = no)               Boxcar smooth the histogram
  (rgrow = 0.)                Region growing radius in scale units
  (mksky = no)                Mark sky annuli on the display
  (mode = "ql")

```

Run daofind, phot.

APPENDIX C

C.1 IRAF commands for psf-fitting photometry

Location: noao/digiphot/daophot

C.1.1 V filter

```
da> lpar datapars
(scale = 1.) Image scale in units per pixel
(fwhmpsf = 3) FWHM of the PSF in scale units
(emission = yes) Features are positive ?
(sigma = 1.3) Standard deviation of background in counts
(datamin = 7.5) Minimum good data value
(datamax = 30000) Maximum good data value
(noise = "poisson") Noise model
(ccdread = "") CCD readout noise image header keyword
(gain = "") CCD gain image header keyword
(readnoise = 15) CCD readout noise in electrons
(epadu = 4) Gain in electrons per count
(exposure = "exptime") Exposure time image header keyword
(airmass = "airmass") Airmass image header keyword
(filter = "filters") Filter image header keyword
(obstime = "utmiddle") Time of observation image header keyword
(itime = 1.) Exposure time
(xairmass = INDEF) Airmass
(ifilter = "INDEF") Filter
(otime = "INDEF") Time of observation
(mode = "ql")
```

```
da> lpar findpars
(threshold = 4.) Threshold in sigma for feature detection
(nsigma = 1.5) Width of convolution kernel in sigma
(ratio = 1.) Ratio of minor to major axis of Gaussian kernel
(theta = 0.) Position angle of major axis of Gaussian kernel
```



```
(sharplo = 0.2) Lower bound on sharpness for feature detection
(sharphi = 1.) Upper bound on sharpness for feature detection
(roundlo = -1.) Lower bound on roundness for feature detection
(roundhi = 1.) Upper bound on roundness for feature detection
(mkdetections = no) Mark detections on the image display ?
(mode = "ql")
```

```
da> lpar centerpars
```

```
(calgorithm = "centroid") Centering algorithm
(cbox = 8.) Centering box width in scale units
(cthreshold = 0.) Centering threshold in sigma above background
(minsnratio = 1.) Minimum signal-to-noise ratio for centering alg
(cmaxiter = 10) Maximum iterations for centering algorithm
(maxshift = 1.) Maximum center shift in scale units
(clean = no) Symmetry clean before centering
(rclean = 1.) Cleaning radius in scale units
(rclip = 2.) Clipping radius in scale units
(kclean = 3.) K-sigma rejection criterion in skysigma
(mkcenter = no) Mark the computed center
(mode = "ql")
```

```
da> lpar photpars
```

```
(weighting = "constant") Photometric weighting scheme
(apertures = 3) List of aperture radii in scale units
(zmag = 25.) Zero point of magnitude scale
(mkapert = no) Draw apertures on the display
(mode = "ql")
```

```
da> lpar fitskypars
```

```
(salgorithm = "mode") Sky fitting algorithm
(annulus = 7.) Inner radius of sky annulus in scale units
(dannulus = 3.) Width of sky annulus in scale units
```

(skyvalue = 0.) User sky value
(smaxiter = 10) Maximum number of sky fitting iterations
(sloclip = 0.) Lower clipping factor in percent
(shiclip = 0.) Upper clipping factor in percent
(snreject = 50) Maximum number of sky fitting rejection iterations
(sloreject = 3.) Lower K-sigma rejection limit in sky sigma
(shireject = 3.) Upper K-sigma rejection limit in sky sigma
(khist = 3.) Half width of histogram in sky sigma
(binsize = 0.1) Binsize of histogram in sky sigma
(smooth = no) Boxcar smooth the histogram
(rgrow = 0.) Region growing radius in scale units
(mksky = no) Mark sky annuli on the display
(mode = "al")

da> lpar daopars

(function = "auto") Form of analytic component of psf model
(varorder = 0) Order of empirical component of psf model
(nclean = 5) Number of cleaning iterations for computing psf
(saturated = no) Use wings of saturated stars in psf model computation
(matchrad = 3.) Object matching radius in scale units
(psfrac = 7.) Radius of psf model in scale units
(fitrad = 3.1) Fitting radius in scale units
(recenter = yes) Recenter stars during fit ?
(fitsky = no) Recompute group sky value during fit ?
(groupsky = yes) Use group rather than individual sky values ?
(sannulus = 0.) Inner radius of sky fitting annulus in scale units
(wsannulus = 11.) Width of sky fitting annulus in scale units
(flaterr = 0.75) Flat field error in percent
(proferr = 5.) Profile error in percent
(maxiter = 50) Maximum number of fitting iterations
(clipexp = 6) Bad data clipping exponent
(cliprange = 2.5) Bad data clipping range in sigma
(mergerad = INDEF) Critical object merging radius in scale units

```
(critsnratio = 1.) Critical S/N ratio for group membership
(maxnstar = 10000) Maximum number of stars to fit
(maxgroup = 60) Maximum number of stars to fit per group
(mode = "ql")
```

C.1.2 B filter

```
da> lpar datapars
(scale = 1.) Image scale in units per pixel
(fwhmpsf = 3.3) FWHM of the PSF in scale units
(emission = yes) Features are positive ?
(sigma = 1) Standard deviation of background in counts
(datamin = 3) Minimum good data value
(datamax = 30000) Maximum good data value
(noise = "poisson") Noise model
(ccdread = "") CCD readout noise image header keyword
(gain = "") CCD gain image header keyword
(readnoise = 15) CCD readout noise in electrons
(epadu = 4) Gain in electrons per count
(exposure = "exptime") Exposure time image header keyword
(airmass = "airmass") Airmass image header keyword
(filter = "filters") Filter image header keyword
(obstime = "utmiddle") Time of observation image header keyword
(itime = 1.) Exposure time
(xairmass = INDEF) Airmass
(ifilter = "INDEF") Filter
(otime = "INDEF") Time of observation
(mode = "ql")
```

```
da> lpar findpars
(threshold = 4.) Threshold in sigma for feature detection
(nsigma = 1.5) Width of convolution kernel in sigma
(ratio = 1.) Ratio of minor to major axis of Gaussian kernel
```

```
(theta = 0.) Position angle of major axis of Gaussian kernel
(sharplo = 0.2) Lower bound on sharpness for feature detection
(sharphi = 1.) Upper bound on sharpness for feature detection
(roundlo = -1.) Lower bound on roundness for feature detection
(roundhi = 1.) Upper bound on roundness for feature detection
(mkdetections = no) Mark detections on the image display ?
(mode = "ql")
```

```
da> lpar centerpars
```

```
(calgorithm = "centroid") Centering algorithm
(cbox = 8.) Centering box width in scale units
(cthreshold = 0.) Centering threshold in sigma above background
(minsnratio = 1.) Minimum signal-to-noise ratio for centering alg
(cmaxiter = 10) Maximum iterations for centering algorithm
(maxshift = 1.) Maximum center shift in scale units
(clean = no) Symmetry clean before centering
(rclean = 1.) Cleaning radius in scale units
(rclip = 2.) Clipping radius in scale units
(kclean = 3.) K-sigma rejection criterion in skysigma
(mkcenter = no) Mark the computed center
(mode = "ql")
```

```
da> lpar photpars
```

```
(weighting = "constant") Photometric weighting scheme
(apertures = 3) List of aperture radii in scale units
(zmag = 25.) Zero point of magnitude scale
(mkapert = no) Draw apertures on the display
(mode = "ql")
```

```
da> lpar fitskypars
```

```
(salgorithm = "mode") Sky fitting algorithm
(annulus = 7.) Inner radius of sky annulus in scale units
```

(dannulus = 3.) Width of sky annulus in scale units
(skyvalue = 0.) User sky value
(smaxiter = 10) Maximum number of sky fitting iterations
(sloclip = 0.) Lower clipping factor in percent
(shiclip = 0.) Upper clipping factor in percent
(snreject = 50) Maximum number of sky fitting rejection iterati
(sloreject = 3.) Lower K-sigma rejection limit in sky sigma
(shireject = 3.) Upper K-sigma rejection limit in sky sigma
(khist = 3.) Half width of histogram in sky sigma
(binsize = 0.1) Binsize of histogram in sky sigma
(smooth = no) Boxcar smooth the histogram
(rgrow = 0.) Region growing radius in scale units
(mksky = no) Mark sky annuli on the display
(mode = "al")

da> lpar daopars

(function = "auto") Form of analytic component of psf model
(varorder = 0) Order of empirical component of psf model
(nclean = 5) Number of cleaning iterations for computing psf
(saturated = no) Use wings of saturated stars in psf model compu
(matchrad = 3.) Object matching radius in scale units
(psfrac = 7.) Radius of psf model in scale units
(fitrad = 3.3) Fitting radius in scale units
(recenter = yes) Recenter stars during fit ?
(fitsky = no) Recompute group sky value during fit ?
(groupsky = yes) Use group rather than individual sky values ?
(sannulus = 0.) Inner radius of sky fitting annulus in scale un
(wsannulus = 11.) Width of sky fitting annulus in scale units
(flaterr = 0.75) Flat field error in percent
(proferr = 5.) Profile error in percent
(maxiter = 50) Maximum number of fitting iterations
(clipexp = 6) Bad data clipping exponent
(cliprange = 2.5) Bad data clipping range in sigma

(mergerad = INDEF) Critical object merging radius in scale units
(critsnratio = 1.) Critical S/N ratio for group membership
(maxnstar = 10000) Maximum number of stars to fit
(maxgroup = 60) Maximum number of stars to fit per group
(mode = "q1")

Run daofind,phot,pstsel,psf,allstar

APPENDIX D

D.1 Standard Stars

The Stetson 2000 catalog was used.

Table D.1

Standard star data

Standard Star	ID	Vcat	Verr	v	Bcat	Berr	b
N5024-S17	214	13.988	0.0052	17.407	14.964	0.0036	18.581
N5024-S22	24	14.274	0.0022	17.728	15.294	0.0061	18.789
N5024-S18	266	14.426	0.0027	17.748	15.31	0.0017	18.916
N5024-S9	135	14.352	0.0022	17.789	15.49	0.0035	19.025
N5024-S4	137	14.432	0.0033	17.833	15.498	0.004	19.066
N5024-S23	26	14.428	0.0023	17.841	15.511	0.0022	18.854
N5024-S8	176	14.572	0.0028	17.979	15.574	0.002	19.047
N5024-S5	268	14.876	0.0043	18.195	15.596	0.0021	19.08
N5024-S20	21	14.935	0.0021	18.391	15.917	0.0018	19.541
N5024-S15	265	15.072	0.0023	18.43	16.025	0.0021	19.521
N5024-S13	81	15.396	0.0039	18.084	16.186	0.0057	19.139

APPENDIX E

E.1 CMD plots of M53 obtained from previous researches

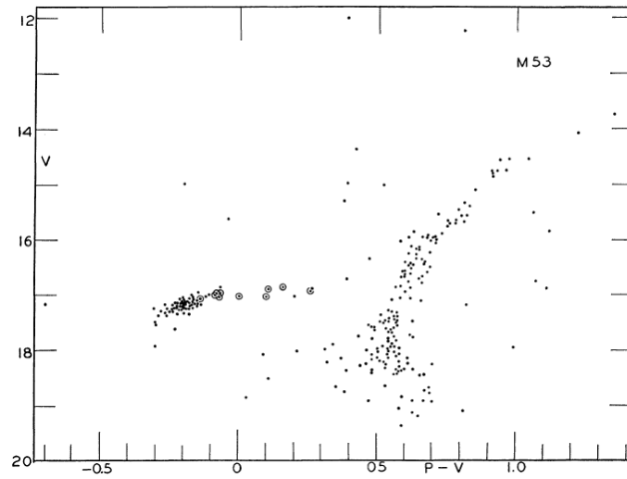


Figure E.1 CMD of M53 ^[12]

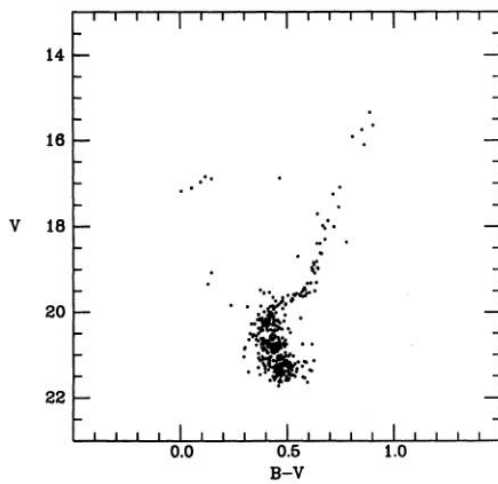


Figure E.2 CMD of M53 ^[13]

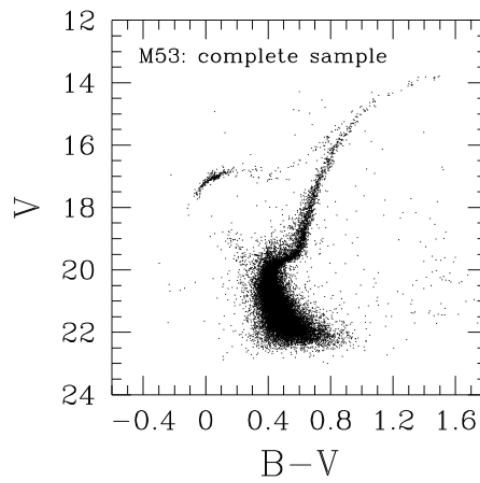


Figure E.3 CMD of M53 ^[14]